Am J Transl Res 2025;17(1):560-584
www.ajtr.org /ISSN:1943-8141/AJTR0158197

Original Article

Comprehensive exploration of signal sequence receptor subunit 1 (SSR1) as a diagnostic and prognostic biomarker in liver hepatocellular carcinoma

Bo Feng[1*], Weixia Chen[1*], Mingyue Sun[1], Xijia Ma[2], Jiarui Cao[2], Zhenyu Zhang[2], Chunzheng Ma[1]

[1]Henan Province Hospital of TCM, Zhengzhou 450002, Henan, China; [2]Henan University of Chinese Medicine, Zhengzhou 450046, Henan, China. [*]Equal contributors.

Received June 1, 2024; Accepted December 5, 2024; Epub January 15, 2025; Published January 30, 2025

Abstract: Objectives: This study investigated the expression, clinical relevance, and functional role of signal sequence receptor 1 (SSR1) in liver hepatocellular carcinoma (LIHC). SSR1's potential as a diagnostic marker and its impact on tumor progression was assessed through multi-platform data analysis and in vitro functional assays. Methodology: Expression data from The Cancer Genome Atlas (TCGA), UALCAN, Oncomine, TIMER2.0, and Human Protein Atlas (HPA) were analyzed to assess SSR1 mRNA and protein expression in LIHC. Clinical correlations with tumor stage, race, gender, age, weight, and nodal metastasis were examined using UALCAN. Promoter methylation, mutation frequency, and prognostic significance were evaluated using UALCAN and OncoDB. Gene set enrichment analysis (GSEA) was conducted to identify pathways enriched in high SSR1 expression. Finally, real-time quantitative polymerase chain reaction (RT-qPCR), proliferation, colony formation, and wound healing assays were performed in QGY-7703 cell lines to validate the SSR1 function. Results: SSR1 was significantly upregulated in LIHC tissues across multiple databases. Promoter hypomethylation was identified as a potential mechanism for this upregulation. High SSR1 expression correlated with worse overall survival and advanced tumor stages. Functional assays revealed that SSR1, SSR2, and SSR3 knockdown in LIHC cells significantly reduced cell proliferation and colony formation while enhancing migratory capacity. Conclusion: SSR1 was overexpressed in LIHC and is associated with poor prognosis. It plays a critical role in promoting LIHC cell proliferation and survival, suggesting its potential as a diagnostic marker and therapeutic target.

Keywords: LIHC, cancer, SSR1, prognosis, treatment

Introduction

Liver cancer is a major global health challenge, ranking as the sixth most common cancer and the third leading cause of cancer-related mortality worldwide [1, 2]. Hepatocellular carcinoma (HCC), also referred to as liver hepatocellular carcinoma (LIHC), accounts for the majority of liver cancer cases, making up approximately 75-85% of all diagnoses [3, 4]. The development of LIHC is closely linked to chronic liver diseases, such as hepatitis B virus (HBV) and hepatitis C virus (HCV) infections, excessive alcohol consumption, and non-alcoholic fatty liver disease (NAFLD), with liver cirrhosis often acting as a precursor [5, 6]. Despite advances in surgical and medical treatments, including liver transplantation, targeted therapies, and immunotherapies, the prognosis for LIHC patients remains poor, particularly in advanced stages [7, 8]. The five-year survival rate for patients diagnosed with late-stage LIHC is less than 20%, underscoring the urgent need for improved diagnostic, prognostic, and therapeutic strategies [9].

A key hurdle in improving LIHC outcomes is the lack of reliable biomarkers for early detection and therapeutic targeting [10]. Currently, available biomarkers, such as alpha-fetoprotein (AFP), have limited sensitivity and specificity, particularly in early-stage disease [11]. This has led to growing interest in identifying novel molecular targets that can be used to improve diagnostic precision and provide new avenues for therapeutic intervention [11]. Among the

https://doi.org/10.62347/ANXV3598

Table 1. Clinical characteristics of LIHC patients (n = 374)

Clinical Characteristics	Number of Patients (n = 374)	Percentage (%)
Gender		
Male	253	67.6%
Female	121	32.4%
Age		
≤ 65 years	177	47.3%
> 60 years	196	52.4%
LIHC Stage		
Stage 1	173	46.3%
Stage 2	87	23.3%
Stage 3	85	22.7%
Stage 4	5	1.3%

LIHC = Liver hepatocellular carcinoma.

emerging molecular candidates, signal sequence receptor 1 (SSR1) has garnered attention for its involvement in protein translocation across the endoplasmic reticulum (ER) membrane, a process critical to maintaining cellular homeostasis [12, 13]. SSR1 is a subunit of the translocon-associated protein (TRAP) complex, which facilitates the movement of newly synthesized proteins into the ER for folding and post-translational modification [14]. Aberrant expression of SSR1 has been reported in several cancers, suggesting it may play a role in tumorigenesis and cancer progression. In breast cancer, SSR1 overexpression has been associated with worse clinical outcomes, including increased tumor size and higher metastatic potential [15]. Similarly, studies in lung and colorectal cancers have indicated that SSR1 contributes to cancer cell survival, proliferation, and metastasis, though the underlying mechanisms remain poorly understood [16, 17].

Despite its implications in other cancers, the role of SSR1 in LIHC has not been comprehensively studied. Given the importance of ER stress and protein homeostasis in cancer progression, SSR1 represents a promising candidate for further investigation in LIHC. In this study, we sought to elucidate the diagnostic, prognostic, and therapeutic relevance of SSR1 in LIHC through a combination of bioinformatic approaches and molecular experiments. Using publicly available cancer databases and in vitro analyses, we aimed to assess the expression patterns of SSR1, its association with clinical outcomes, and its potential as a therapeutic target in LIHC.

Our findings provide new insights into the role of SSR1 in liver cancer, highlighting its potential as a biomarker for diagnosis and prognosis, as well as a therapeutic target for intervention. By integrating bioinformatics data with experimental validation, this study contributes to the growing body of knowledge on the molecular underpinnings of LIHC and lays the groundwork for future research into SSR1 as a novel therapeutic avenue for liver cancer management.

Methodology

Data acquisition from The Cancer Genome Atlas (TCGA) database

Gene expression data from LIHC studies were collected using the TCGA database (https://cancergenome.nih.gov). Datasets included 50 normal and 374 tumor tissues (**Table 1**), with a workflow type of transcript per million (TPM).

UALCAN, Oncomine, TIMER2.0 and Human Protein Atlas (HPA) databases

UALCAN, Oncomine, TIMER2.0, and HPA are widely used bioinformatics platforms for cancer research. UALCAN (https://ualcan.path.uab.edu/) provides access to TCGA data, enabling researchers to analyze gene expression, promoter methylation, and survival rates across cancer types [18]. Oncomine (http://www.oncomine.org) offers a comprehensive collection of cancer transcriptome data, allowing for comparative gene expression analysis across various tumors and normal tissues [19]. TIMER2.0 (http://timer.cistrome.org/) focuses on tumor immune infiltration, helping users study the association between immune cells and cancer prognosis, gene expression, and somatic mutations [20]. The HPA (https://www.proteinatlas.org/) presents data on tissue-specific protein expression, helping researchers link protein levels with histological and pathological data across normal and cancerous tissues, offering insights into the roles of specific genes in cancer biology [21]. In the present study, UALCAN, Oncomine, TIMER2.0, and HPA databases were utilized to analyze the SSR1 gene expression across different large cohorts of LIHC patients. Moreover, UALCAN was also

used to analyze the promoter methylation level of SSR1 across LIHC.

OncoDB database

OncoDB (https://oncodb.org/) is a cancer genomics database that integrates multi-omics data, including mutations, gene expression, copy number variations, and survival outcomes across various cancer types [22]. It provides researchers with tools for analyzing gene alterations, exploring tumor heterogeneity, and identifying potential biomarkers or therapeutic targets, making it a valuable resource for precision oncology and cancer biology studies. Here, in this study we used the OncoDB database to conduct mutational analysis of the SSR1 gene across LIHC tissues samples.

Prognostic significance of SSR1

The prognostic significance of SSR1 for overall survival was first evaluated using data from 374 LIHC patients retrieved from the TCGA database. Next, the GENT2 database (http://gent2.appex.kr/gent2/) was used to create a forest plot summarizing SSR1 survival data from multiple studies. GENT2 is a user-friendly database that provides gene expression data from various cancer and normal tissues [23]. It allows researchers to explore differential gene expression, survival analysis, and generate visualizations like forest plots, aiding in the discovery of potential cancer biomarkers.

Gene set enrichment analysis (GSEA)

GSEA, a computational method, evaluates the statistical significance and consistent variations in predefined gene sets between two biological conditions. Genes linked to SSR1 expression from recent studies was identified using GSEA. It also examined survival differences between high- and low-SSR1 expression groups, with 1,000 gene set permutations. Gene sets were considered significant with $P < 0.05$ and a false discovery rate (FDR) < 25%.

Immune infiltration and drug sensitivity analyses of SSR1

GSCA (Gene Set Cancer Analysis, https://guolab.wchscu.cn/GSCA), developed by Guo Lab, is an integrative platform for analyzing cancer genomics data [24]. It provides tools for exploring gene set enrichment, mutation analysis, and drug sensitivity across various cancers. GSCA helps identify key genetic alterations, potential therapeutic targets, and drug response patterns in cancer research. This study utilized the GSCA database to perform immune infiltration and drug sensitivity analyses of SSR1.

Protein-protein interaction (PPI) network construction and correlation analysis

The STRING (Search Tool for the Retrieval of Interacting Genes/Proteins) database (https://string-db.org/) is a comprehensive resource that provides information on known and predicted protein-protein interactions [25]. It integrates data from various sources to support the functional interpretation of complex biological networks. In this work, the STRING database was utilized to construct the PPI network of SSR1-related proteins.

GEPIA2 (Gene Expression Profiling Interactive Analysis 2, http://gepia2.cancer-pku.cn/#index) is a web-based tool for analyzing RNA sequencing expression data from TCGA and the Genotype-Tissue Expression (GTEx) projects [26]. It offers customizable analyses such as differential expression, survival analysis, and correlation analysis, providing an accessible platform for exploring cancer genomics. This study utilized the GEPIA2 database to explore correlations between SSR1 and its other associated genes.

Correlations of SSR1 with immune and molecular subtypes of LIHC

TISIDB (http://cis.hku.hk/TISIDB/index.php) is an integrated database designed to analyze tumor-immune system interactions [27]. It consolidates data from various resources, including TCGA and PubMed, to provide insights into immune genes, lymphocytes, immunomodulators, and chemokines. Researchers use TISIDB to explore immune infiltration, biomarkers, and therapeutic targets across cancer types. We utilized the TISIDB database to investigate SSR1 correlations with immune and molecular subtypes, along with its associations with immune inhibitor and stimulator genes.

Cell lines and culture conditions

Seven LIHC cell lines, QGY-7703, Huh7, SNU-449, SNU-475, PLC/PRF/5, Hep3B, and SMMC-

7721, and three normal liver cell lines, THLE-2, THLE-3, and MIHA, were purchased from the American Type Culture Collection (ATCC, USA). All cell lines were cultured in complete medium, consisting of Dulbecco's Modified Eagle Medium (DMEM; Thermo Fisher Scientific, Catalog #11965092) supplemented with 10% fetal bovine serum (FBS; Thermo Fisher Scientific, Catalog #26140079) and 1% penicillin-streptomycin (Thermo Fisher Scientific, Catalog #15070063), under standard conditions at 37°C in a humidified incubator with 5% CO_2. The medium was changed every two days, and cells were sub-cultured at 80% confluence using TrypLE Express (Thermo Fisher Scientific, Catalog #12604021).

Real-time quantitative polymerase chain reaction (RT-qPCR) analysis of SSR1 and other associated genes

Total RNA was extracted from the seven LIHC cell lines (HepG2, Huh7, SNU-449, SNU-475, PLC/PRF/5, Hep3B, SK-HEP-1) and three normal liver cell lines (THLE-2, THLE-3, MIHA) using the PureLink™ RNA Mini Kit (Thermo Fisher Scientific, Catalog #12183018A) following the manufacturer's instructions. The quality and quantity of RNA were assessed using a NanoDrop™ 2000 spectrophotometer (Thermo Fisher Scientific). cDNA synthesis was performed using the High-Capacity cDNA Reverse Transcription Kit (Thermo Fisher Scientific, Catalog #4368814). Briefly, 1 μg of RNA was reverse transcribed in a reaction volume of 20 μL according to the kit protocol.

RT-qPCR was carried out to assess the expression levels of SSR1, SSR2, SSR3, SSR4, RPN1, and SEC61A1 using TaqMan™ Gene Expression Assays (Thermo Fisher Scientific, Assay IDs: SSR1 - Hs00419565_m1, SSR2 - Hs00912856_m1, SSR3 - Hs00212973_m1, SSR4 - Hs00192559_m1, RPN1 - Hs00264494_m1, SEC61A1 - Hs00917535_m1). Reactions were performed using the TaqMan™ Universal Master Mix II (Thermo Fisher Scientific, Catalog #4440040) on an Applied Biosystems™ QuantStudio™ 5 Real-Time PCR System (Thermo Fisher Scientific). Each reaction was performed in a 20 μL volume containing 10 μL of TaqMan™ Universal Master Mix, 1 μL of TaqMan™ gene expression assay, and 9 μL of diluted cDNA template. Gene expression was normalized to the housekeeping gene GAPDH (TaqMan™ Assay ID: Hs02786624_g1), and relative expression levels were calculated using the $2^{-\Delta\Delta Ct}$ method.

SSR1, SSR2, and SSR3 knockdown

QGY-7703 and SMMC-7721 cells were transfected with specific siRNA duplexes targeting SSR1 (5'-AGAAAACAAGGGUUUUGGCAA-3'), SSR2 (5'-CUUCUUGACUGCUAAGGGAUU-3'), and SSR3 (5'-GAACCUACUUGUCCGAUAAUU-3'), sourced from RiboBio (Guangzhou, China). The knockdown of SSR1 was performed in both QGY-7703 and SMMC-7721 cells, whereas SSR2 and SSR3 knockdowns were exclusively conducted in QGY-7703 cells. Transfections were carried out using Lipofectamine™ RNAiMAX Transfection Reagent (Thermo Fisher Scientific, Catalog #13778075), following the manufacturer's protocol. For each transfection, 7.5 μL of Lipofectamine™ RNAiMAX was initially diluted in 250 μL of Opti-MEM™ Reduced Serum Medium (Thermo Fisher Scientific, Catalog #31985062) and incubated for 5 minutes at room temperature to prepare the lipid mixture. Separately, 25 pmol of SSR1, SSR2, and SSR3 siRNA duplexes were diluted in an additional 250 μL of Opti-MEM™. The diluted siRNA was then combined with the prepared Lipofectamine™ RNAiMAX solution and incubated at room temperature for 20 minutes, allowing the formation of siRNA-lipid complexes. For each target, the siRNA-lipid complexes were added dropwise to the designated cells in 6-well plates, ensuring even distribution across the well surface. After adding the complexes, cells were incubated at 37°C in a humidified atmosphere containing 5% CO_2 for 48 hours.

Following the 48-hour incubation, the knockdown efficiency of SSR1, SSR2, and SSR3 was evaluated by RT-qPCR and Western blot analyses. RT-qPCR was performed utilizing aforementioned conditions. While for Western blot, cells were lysed using RIPA buffer (Thermo Fisher, #89901) with protease/phosphatase inhibitors (#78441). Lysates were centrifuged at 12,000 × g for 15 minutes at 4°C, and protein concentrations were quantified using the BCA Protein Assay Kit (#23225). Equal amounts (20-30 μg) of protein were denatured, separated on SDS-PAGE, and transferred to PVDF membranes (#88518). Membranes were blocked with 5% milk in TBS-T, then incubated overnight at 4°C with primary antibodies for

SSR1 (Thermo Fisher Scientific, Catalog # TA503263), SSR2 (Thermo Fisher Scientific, Catalog # PA5-120727), SSR3 (Thermo Fisher Scientific, Catalog # PA5-80072), and GAPDH (Thermo Fisher Scientific, Catalog # MA5-35235) as the loading control. After washing, membranes were incubated with HRP-conjugated secondary antibodies for 1 hour, and bands were visualized with ECL substrate (#32106). Protein levels were quantified by densitometry using ImageJ, normalized to GAPDH, to confirm SSR1, SSR2, and SSR3 knockdown.

Cell proliferation assay

Cell proliferation was assessed using the Cell Counting Kit-8 (CCK-8; Thermo Fisher Scientific, Catalog #A31174). After 48 hours of siRNA transfection, QGY-7703 and SMMC-7721 cells were harvested and seeded into 96-well plates at a density of 2,000 cells per well in 100 µL of complete medium. Cells were incubated for 0, 24, 48, and 72 hours at 37°C with 5% CO_2. At each time point, 10 µL of CCK-8 reagent was added to each well, and the plates were incubated for 2 hours. Absorbance was measured at 450 nm using a microplate reader (Thermo Fisher Scientific, Catalog #51119000) to determine cell viability.

Colony formation assay

To assess the long-term proliferation potential, a colony formation assay was performed. After siRNA transfection, QGY-7703 and SMMC-7721 cells were seeded in 6-well plates at a density of 500 cells per well in 2 mL of complete medium. The cells were incubated at 37°C with 5% CO_2 for 10-14 days until visible colonies formed. The medium was replaced every 3 days. At the end of the incubation period, the colonies were fixed with 4% paraformaldehyde (Thermo Fisher Scientific, Catalog #28908) for 15 minutes and stained with 0.1% crystal violet solution (Thermo Fisher Scientific, Catalog #R40052) for 30 minutes. Colonies containing at least 30 cells were counted under a microscope, and colony numbers were quantified.

Wound healing assay

The wound healing assay was used to evaluate cell migration. After siRNA transfection, QGY-7703 and SMMC-7721 cells were seeded into 6-well plates and grown to 90-100% confluence in a complete medium. A uniform scratch was made in the cell monolayer using a sterile 200 µL pipette tip. The cells were then washed twice with phosphate-buffered saline (PBS; Thermo Fisher Scientific, Catalog #10010023) to remove detached cells and debris, and a fresh serum-free medium was added. Images of the wound were taken at 0 and 24 hours using a phase-contrast microscope (Thermo Fisher Scientific). The wound area was measured using ImageJ software, and the percentage of wound closure was calculated.

Statistics

Box plots were used to evaluate gene expression levels in LIHC. The association between clinical characteristics and SSR1 expression was analyzed using the Wilcoxon signed-rank test and logistic regression. The Kaplan-Meier method, along with the log-rank test, was applied to compare overall survival (OS) rates between groups with high and low SSR1 levels. Diagnostic values were assessed using receiver operating characteristic (ROC) curves, with the area under the curve (AUC) indicating diagnostic performance. All statistical analyses were conducted using R statistical software (version 3.5.3) or SPSS software (version 24.0), with significance thresholds set at *P < 0.05, **P < 0.01, and ***P < 0.001.

Results

High SSR1 expression in LIHC

Firstly, the expression analysis of SSR1 was performed using expression data from various authentic sources. In **Figure 1A**, data from the TCGA database showed a significant upregulation of SSR1 expression in tumor samples (n = 374) compared to normal tissue (n = 50). **Figure 1B** further substantiates this finding using the UALCAN database, comparing SSR1 expression in normal (n = 50) and primary tumor (n = 371) samples. Once again, SSR1 was significantly upregulated in tumor tissues, strengthening the evidence of its involvement in LIHC pathology. In **Figure 1C**, data from the Oncomine database (Roessler Liver 2 dataset) shows a similar trend. SSR1 expression was significantly higher in LIHC samples compared to normal liver tissue (**Figure 1C**). **Figure 1D** uses the TIMER2.0 platform to analyze SSR1 expression

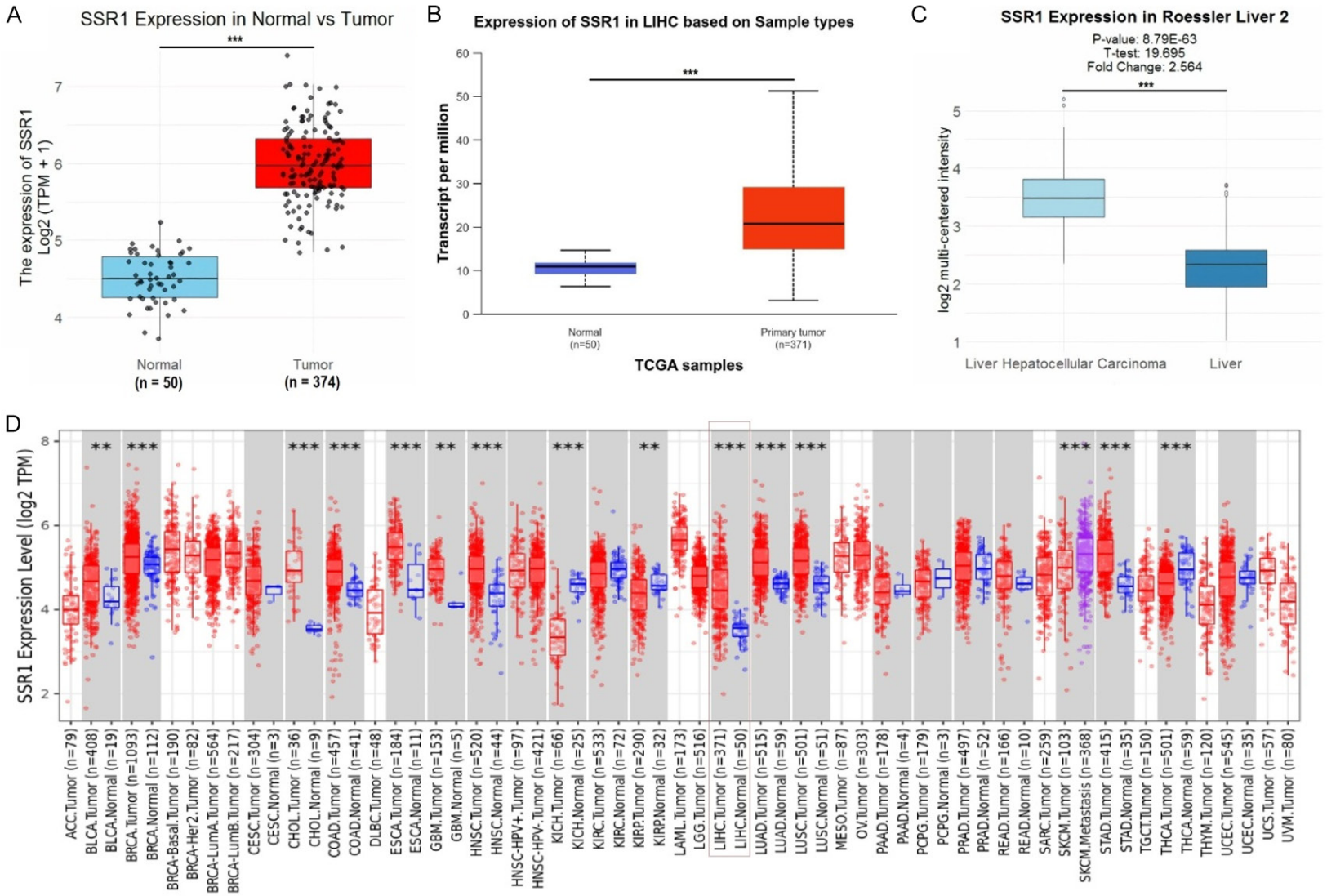
A
SSR1 Expression in Normal vs Tumor
***
The expression of SSR1 Log2 (TPM + 1)
Normal (n = 50)
Tumor (n = 374)
B
Expression of SSR1 in LIHC based on Sample types
***
Transcript per million
Normal (n=50)
Primary tumor (n=371)
TCGA samples
C
SSR1 Expression in Roessler Liver 2
P-value: 8.79E-63
T-test: 19.695
Fold Change: 2.564
***
log2 multi-centered intensity
Liver Hepatocellular Carcinoma
Liver
D
SSR1 Expression Level (log2 TPM)
ACC.Tumor (n=79)
BLCA.Tumor (n=408)
BLCA.Normal (n=19)
BRCA.Tumor (n=1093)
BRCA.Normal (n=112)
BRCA-Basal.Tumor (n=190)
BRCA-Her2.Tumor (n=82)
BRCA-LumA.Tumor (n=564)
BRCA-LumB.Tumor (n=217)
CESC.Tumor (n=304)
CESC.Normal (n=3)
CHOL.Tumor (n=36)
CHOL.Normal (n=9)
COAD.Tumor (n=457)
COAD.Normal (n=41)
DLBC.Tumor (n=48)
ESCA.Tumor (n=184)
ESCA.Normal (n=11)
GBM.Tumor (n=153)
GBM.Normal (n=5)
HNSC.Tumor (n=520)
HNSC.Normal (n=44)
HNSC-HPV+.Tumor (n=97)
HNSC-HPV-.Tumor (n=421)
KICH.Tumor (n=66)
KICH.Normal (n=25)
KIRC.Tumor (n=533)
KIRC.Normal (n=72)
KIRP.Tumor (n=290)
KIRP.Normal (n=32)
LAML.Tumor (n=173)
LGG.Tumor (n=516)
LIHC.Tumor (n=371)
LIHC.Normal (n=50)
LUAD.Tumor (n=515)
LUAD.Normal (n=59)
LUSC.Tumor (n=501)
LUSC.Normal (n=51)
MESO.Tumor (n=87)
OV.Tumor (n=303)
PAAD.Tumor (n=178)
PAAD.Normal (n=4)
PCPG.Tumor (n=179)
PCPG.Normal (n=3)
PRAD.Tumor (n=497)
PRAD.Normal (n=52)
READ.Tumor (n=166)
READ.Normal (n=10)
SARC.Tumor (n=259)
SKCM.Tumor (n=103)
SKCM.Metastasis (n=368)
STAD.Tumor (n=415)
STAD.Normal (n=35)
TGCT.Tumor (n=150)
THCA.Tumor (n=501)
THCA.Normal (n=59)
THYM.Tumor (n=120)
UCEC.Tumor (n=545)
UCEC.Normal (n=35)
UCS.Tumor (n=57)
UVM.Tumor (n=80)

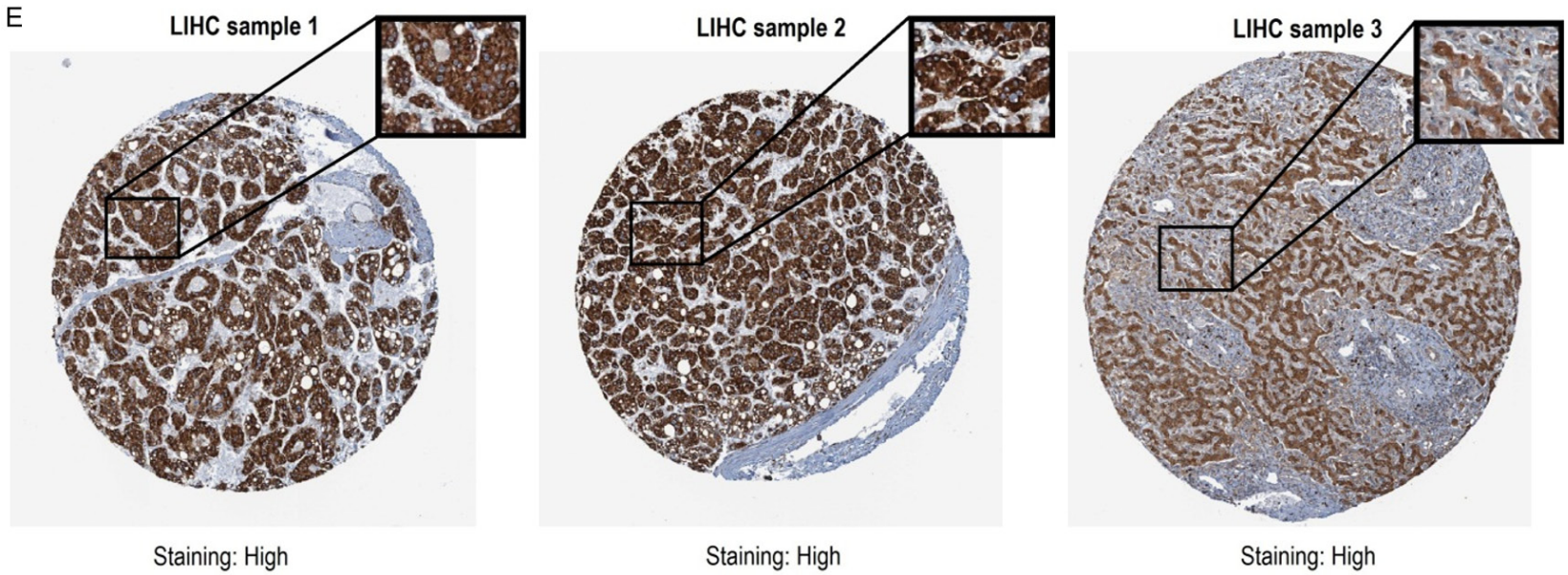

Figure 1. Elevated expression of signal sequence receptor 1 (SSR1) in liver hepatocellular carcinoma (LIHC) across multiple datasets. A. The expression of SSR1 in LIHC samples compared to normal liver tissues using data from The Cancer Genome Atlas (TCGA). B. SSR1 expression comparison between normal liver tissues and primary tumors in LIHC, visualized via UALCAN database. C. Expression analysis of SSR1 using the Oncomine platform. D. Pan-cancer analysis of SSR1 expression across various cancer types using TIMER2.0. E. Immunohistochemical staining of SSR1 in three different LIHC tissue samples from the Human Protein Atlas (HPA) database, showing high SSR1 expression levels (brown staining) across all samples. **P < 0.01 and ***P < 0.001.

across various tumor types. SSR1 appears to be upregulated in multiple cancer types, including LIHC, further emphasizing its potential as a pan-cancer marker (**Figure 1D**). Lastly, **Figure 1E** illustrates immunohistochemistry (IHC) results from the HPA, showing high levels of SSR1 staining in three representative LIHC tissue samples. The staining is predominantly strong, suggesting a high protein expression level of SSR1 in LIHC tissues (**Figure 1E**), which aligns with the transcriptomic data presented in the earlier panels. Together, these analyses strongly suggest that SSR1 was overexpressed in LIHC at both mRNA and protein levels, which may point to its potential role as a diagnostic marker.

Correlations of SSR1 with different clinical variables of LIHC

Correlations of SSR with different clinical variables of LIHC were evaluated using the UALCAN database. Across different cancer stages, SSR1 expression was significantly higher in all stages (Stage 1 through Stage 4) compared to normal tissue, with a progressive increase in expression from Stage 1 to Stage 4, indicating that SSR1 is upregulated early in tumorigenesis and remains elevated throughout disease progression (**Figure 2A**). When examining SSR1 expression based on race, there was a significant increase in SSR1 levels in LIHC patients from all racial groups (Caucasian, African-American, and Asian) compared to normal tissues (**Figure 2B**). For gender, SSR1 expression was significantly higher in both males and females with LIHC compared to normal tissues (**Figure 2C**). With respect to age, all age groups (21-40 years, 41-60 years, 61-80 years, and 81-100 years) showed significantly elevated SSR1 levels compared to normal tissues (**Figure 2D**). In terms of weight, SSR1 was consistently upregulated across all weight categories (normal weight, extreme weight, obese, and extreme obese) compared to normal tissues (**Figure 2E**). Finally, in relation to nodal metastasis status, both the N0 (no lymph node metastasis) and N1 (presence of lymph node metastasis) groups show significantly higher SSR1 expression compared to normal tissues (**Figure 2F**). Although SSR1 levels are slightly higher in the N1 group than in N0, the upregulation in both groups suggests that SSR1 plays a role in LIHC, regardless of metastatic involvement (**Figure 2F**). In summary, SSR1 was consistently overexpressed in LIHC across various clinical parameters, including cancer stage, race, gender, age, weight, and nodal metastasis status.

Promoter methylation level of SSR1 in LIHC

The promoter methylation analysis of SSR1 in LIHC was analyzed using the UALCAN database. Overall, the promoter methylation level of SSR1 in primary LIHC samples was significantly lower than in normal tissues (**Figure 3A**). This suggests that SSR1 is subject to promoter hypomethylation in LIHC, potentially leading to its overexpression. When stratified by cancer stages, a decrease in SSR1 promoter methylation was observed in all stages (Stage 1 through Stage 4) compared to normal tissues (**Figure 3B**). In terms of race, all groups (Caucasian, African-American, and Asian) exhibited significantly lower SSR1 promoter methylation compared to normal tissues (**Figure 3C**). Regarding gender, SSR1 promoter methylation was significantly lower in both males and females with LIHC compared to normal controls (**Figure 3D**). The analysis based on age revealed that all age groups (21-40, 41-60, 61-80, and 81-100 years) had significantly lower promoter methylation levels in tumor tissues compared to normal tissues (**Figure 3E**). In terms of weight, SSR1 promoter methylation was significantly lower in all weight categories (normal weight, extreme weight, obese, and extreme obese) of LIHC patients compared to normal tissues (**Figure 3F**). In summary, SSR1 promoter methylation was consistently lower in LIHC across all examined clinical variables, including cancer stage, race, gender, age, and weight, compared to normal tissues.

Mutational analysis of SSR1 in LIHC

The mutational analysis of SSR1 in LIHC was conducted using combined DNA-seq and RNA-seq data from the OncoDB database. The results indicated that one patient had a mutation in SSR1, corresponding to a mutation frequency of 0.3% out of a total of 373 patients (**Figure 4**). The analysis further identified the mutation subtype as a missense mutation (N136T) (**Figure 4**). This mutation occurred within the TRAP_alpha domain of the SSR1 protein (**Figure 4**). No other mutations were detected in this analysis of the patient cohort.

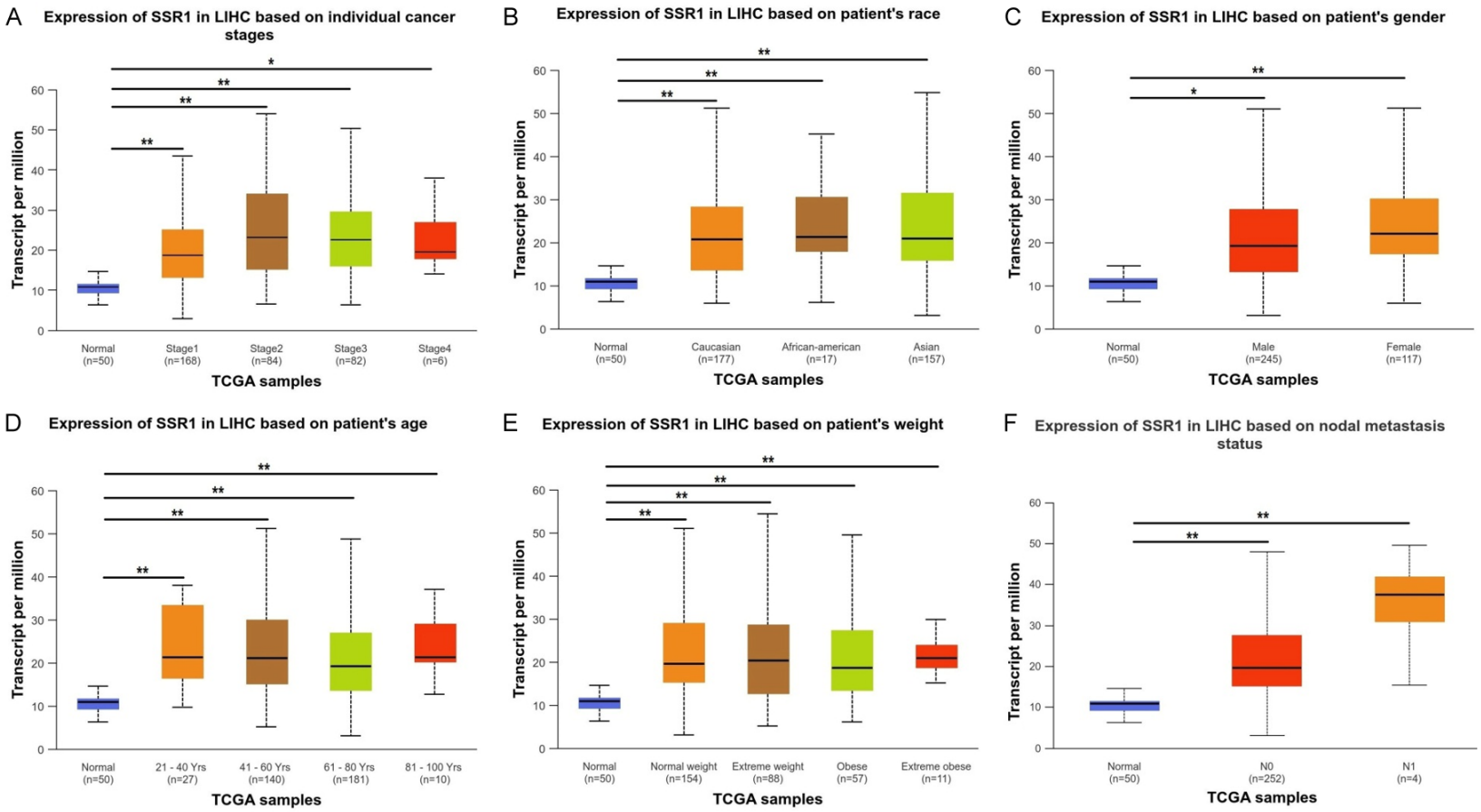

Figure 2. Correlation of signal sequence receptor 1 (SSR1) expression with clinical variables in liver hepatocellular carcinoma (LIHC) based on UALCAN analysis. A. Expression of SSR1 in different cancer stages of LIHC. B. SSR1 expression in LIHC based on the patient's race. C. SSR1 expression in LIHC based on the patient's gender. D. SSR1 expression in LIHC based on the patient's age. E. SSR1 expression in LIHC based on the patient's weight. F. SSR1 expression based on nodal metastasis status. *P < 0.05 and **P < 0.01.

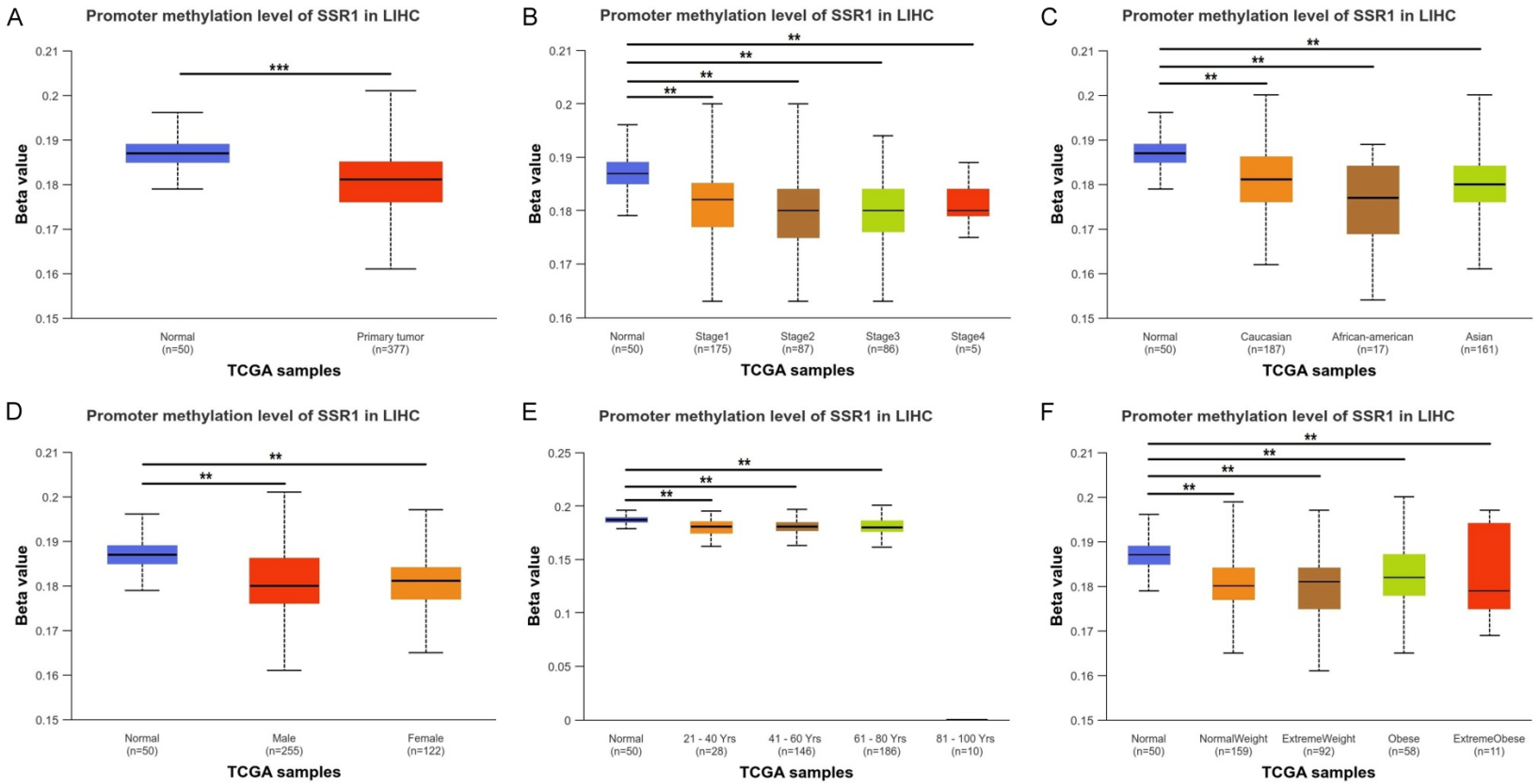

Figure 3. Promoter methylation analysis of signal sequence receptor 1 (SSR1) in liver hepatocellular carcinoma (LIHC) based The Cancer Genomics Altas (TCGA) data via the UALCAN analysis. A. Promoter methylation levels of SSR1 in normal and primary tumor LIHC samples. B. Methylation levels of SSR1 in different cancer stages of LIHC. C. Methylation levels of SSR1 in LIHC based on the patient's race. D. SSR1 methylation levels in LIHC based on the patient's gender. E. Promoter methylation of SSR1 in LIHC based on the patient's age. F. Methylation levels of SSR1 in LIHC based on the patient's weight. *P < 0.05, **P < 0.01, and ***P < 0.001.

SSR1 mutations in LIHC by combined DNA-seq and RNA-seq analyses

Gene	Cancer type	num of patients with mutation	mutation frequency	Total patients
SSR1	LIHC	1	**0.3%**	373

SSR1 mutation subtypes in LIHC by combined DNA-seq and RNA-seq analyses

Gene	Cancer type	Mutation type	num of patients with mutation	mutation frequency	Total patients
SSR1	LIHC	Missense_Mutation	1	0.3%	373

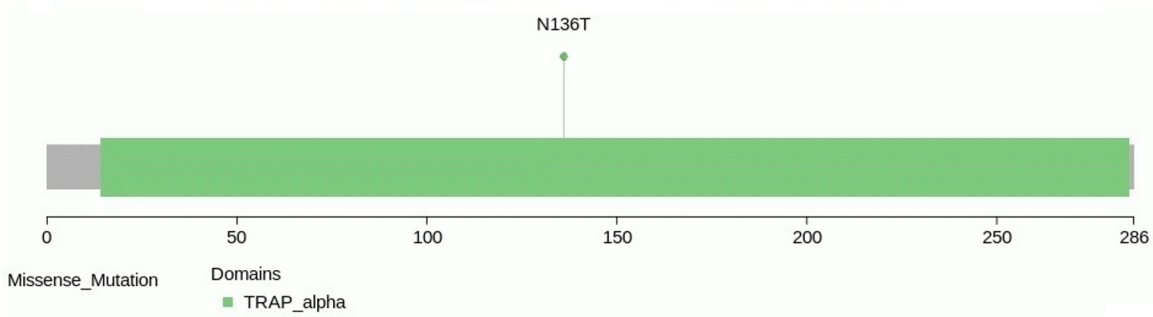

Figure 4. Signal sequence receptor 1 (SSR1) mutations across liver hepatocellular carcinoma (LIHC) tissue samples by combined DNA sequencing (DNA-seq) and RNA sequencing (RNA-seq) analyses. The figure shows the mutation analysis of SSR1 in LIHC, highlighting one missense mutation, N136T, in a sample of 373 patients.

Prognostic significance of SSR1 in LIHC

Initially, the survival analysis of SSR1 was performed using data from 374 patients in TCGA. KM survival curves in **Figure 5A** to **5I** depict the relationship between SSR1 expression levels (high and low) and overall survival across different patient subgroups. In **Figure 5A**, high SSR1 expression was associated with worse overall survival (HR = 1.55, log-rank P = 0.012). **Figure 5B** shows that high SSR1 expression was also linked to poorer survival (HR = 1.47, log-rank P = 0.035) in patients with T1, T2, and T3 stage tumors. Similarly, **Figure 5C** highlighted worse outcomes in patients with T3 and T4 stage tumors (HR = 1.67, log-rank P = 0.049). Patients with stage I, II, III, and IV tumors exhibited significantly lower survival with high SSR1 expression (HR = 1.51, log-rank P = 0.026) (**Figure 5D**), and similar results were seen in patients with stages I, II, and III tumors (HR = 1.49, log-rank P = 0.032) (**Figure 5E**). **Figure 5F** demonstrated a significant decrease in survival in patients with high SSR1 expression and poor histologic grades (G2 and G3) (HR = 1.70, log-rank P = 0.003). **Figure 5G** showed a particularly strong association between high SSR1 expression and poor survival in patients with G1 histologic grade (HR = 3.45, log-rank P = 0.007). Further analysis in **Figure 5H** and **5I** revealed that male patients (HR = 2.06, log-rank P = 0.001) and patients aged over 60 (HR = 1.61, log-rank P = 0.037) with high SSR1 expression had significantly poorer survival outcomes. **Figure 5J** presents a forest plot summarizing the hazard ratios (HR) from multiple studies using the GENT2 database. The overall analysis revealed that high SSR1 expression had a slightly unfavorable effect on survival (HR = 0.96) (**Figure 5J**). The fixed-effect and random-effects models yielded similar results, with a *p*-value of 0.037 (**Figure 5J**), indicating moderate heterogeneity across the studies.

GSEA analysis

We performed GSEA using datasets with low and high SSR1 expression to identify activated signaling pathways in LIHC. Gene sets linked to processes such as “cell cycle”, “neuroactive ligand receptor interaction”, “axon guidance”, “gap junction”, “DNA replication”, “gamma R-mediated phagocytosis”, “ECM receptor interaction”, “TGF-β signaling pathway”, and the “N-cadherin pathway” in LIHC showed notable enrichment in the high SSR1 expression phenotype, as illustrated in **Figure 6A-I**.

Correlations of SSR1 with immune infiltration, drug sensitivity, and related genes

The correlations of SSR1 with immune infiltration and drug sensitivity were analyzed using

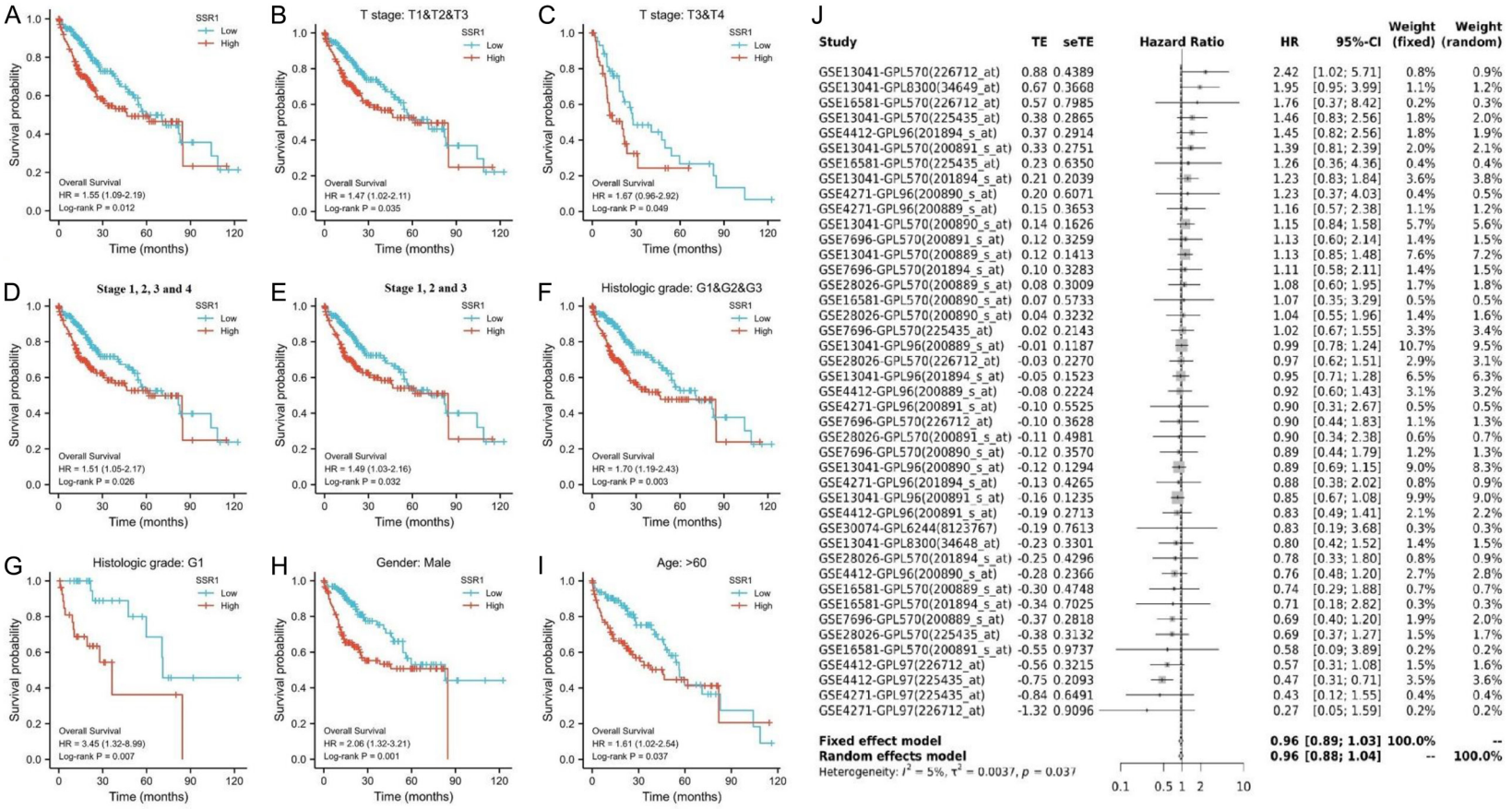

Figure 5. Kaplan-Meier survival curves for signal sequence receptor 1 (SSR1) expression in liver hepatocellular carcinoma (LIHC) based on various clinical parameters. Data was derived from 374 LIHC samples from The Cancer Genome Atlas (TCGA) database, categorized by (A) SSR1 expression, (B) T stage (T1, T2, and T3), (C) T stage (T3 and T4), (D) clinical stage (1, 2, 3, and 4), (E) clinical stage (1, 2, and 3), (F) histologic grade (G1 and G2 vs. G3), (G) histologic grade (G1), (H) gender (male), and (I) age (> 60). (J) Shows a GENT2-based forest plot of hazard ratios (HR) across multiple studies analyzing SSR1 expression in various LIHC datasets. $P < 0.05$.

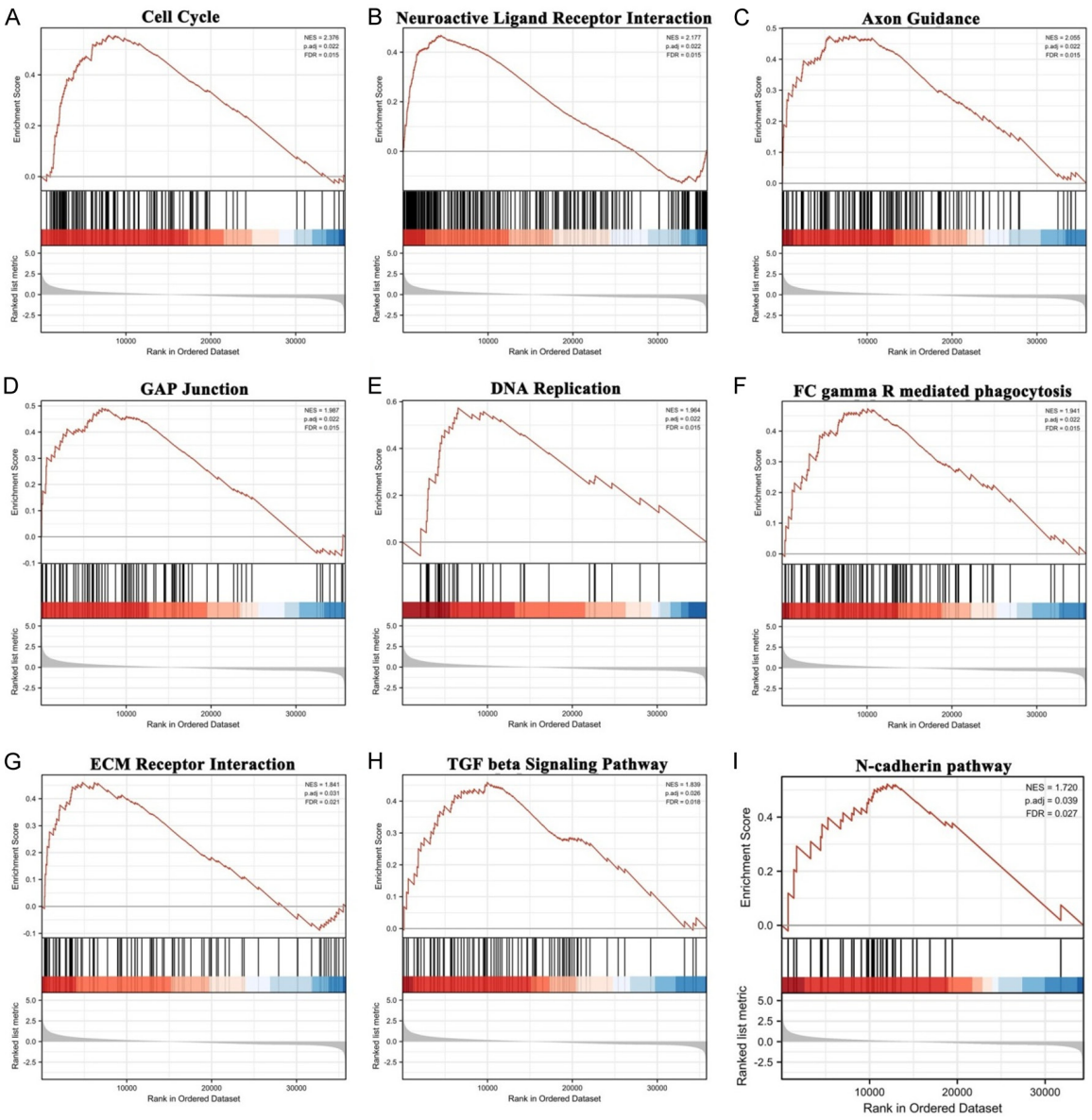

Figure 6. Gene set enrichment analysis (GSEA) plots. Enrichment plots for the following pathways in liver hepatocellular carcinoma (LIHC) cases with high signal sequence receptor 1 (SSR1) expression: (A) Cell cycle, (B) Neuroactive ligand-receptor interaction, (C) Axon guidance, (D) GAP junction, (E) DNA replication, (F) FC gamma R-mediated phagocytosis, (G) ECM-receptor interaction, (H) TGF-beta signaling pathway, and (I) N-cadherin pathway. $P < 0.05$.

the GSCA database. In **Figure 7A**, SSR1 expression demonstrated both positive and negative correlations with different immune cell types in LIHC. Positive correlations (marked in red) were observed with CD8+ T cells, Tregs, and CD4+ T cells, indicating that higher SSR1 expression is associated with increased infiltration of these immune cells (**Figure 7A**). In contrast, negative correlations (shown in blue) were found with cell types such as Th1 and monocytes, suggesting lower immune cell infiltration with increased SSR1 expression (**Figure 7A**).

In **Figure 7B**, the analysis explored the correlation between SSR1 expression and drug sensitivity using the GDSC dataset. While most drugs exhibited minimal correlations, some noteworthy patterns emerged. There were weak negative correlations (blue) between SSR1 expression and sensitivity to AZ628, Lapatinib, and Crizotinib, meaning that higher SSR1 expression may be linked to enhanced sensitivity to these drugs (**Figure 7B**). Conversely, positive correlations (red) were observed for Afatinib and Erlotinib, suggesting that increased SSR1

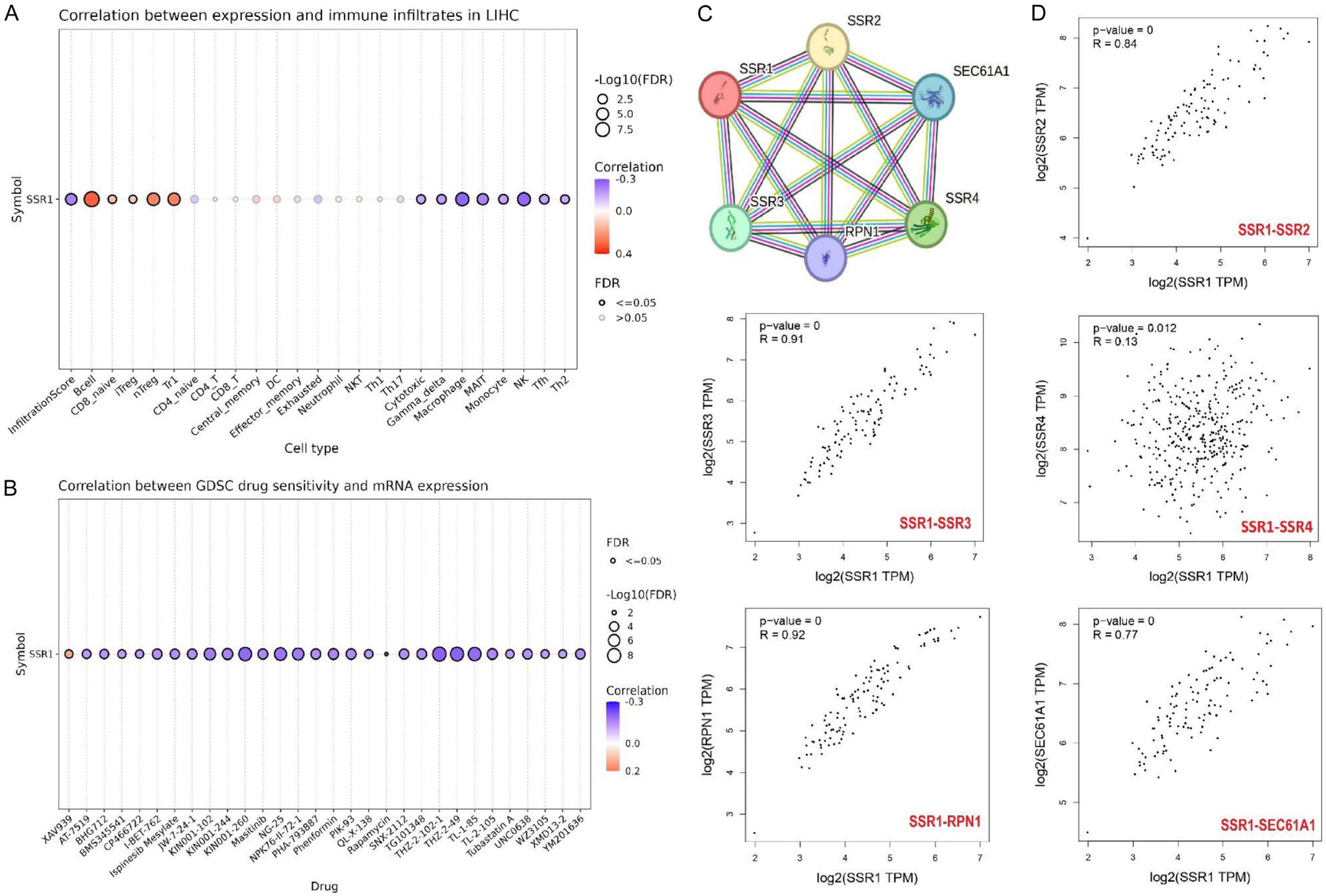

Figure 7. Correlation analysis of for signal sequence receptor 1 (SSR1) expression with immune infiltration, drug sensitivity, and co-expression in liver hepatocellular carcinoma (LIHC). A. Correlation between SSR1 expression and various immune cell infiltrates in hepatocellular carcinoma (LIHC), analyzed using the GSCA database. B. Correlation between SSR1 mRNA expression and drug sensitivity for different cancer drugs, also analyzed using the GSCA database. C. Protein-protein interaction network involving SSR1, created using the Search tool for the retrieval of interacting genes/proteins (STRING) database. D. Scatter plots showing pairwise correlations of SSR1 with SSR2, SSR3, RPN1, and SEC61A1 at the mRNA expression level in LIHC samples, analyzed using GEPIA2. $P < 0.05$.

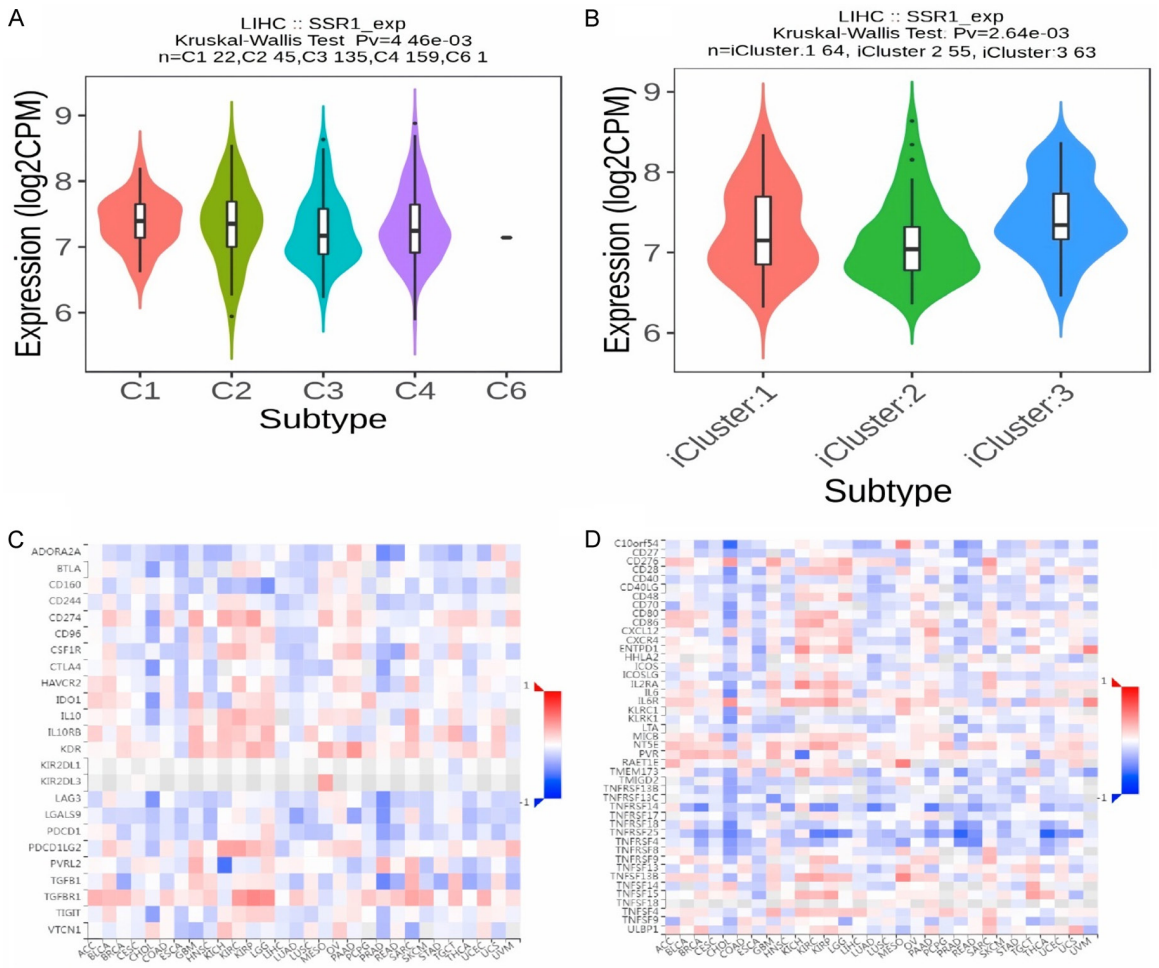

Figure 8. Differential expression of signal sequence receptor 1 (SSR1) in immune and molecular subtypes of liver hepatocellular carcinoma (LIHC) and its correlation with immune inhibitors and stimulators. (A) Violin plot showing SSR1 expression across immune subtypes (C1-C6) in LIHC. (B) Violin plot illustrating SSR1 expression across molecular subtypes (iCluster 1 to 3). (C) Heatmap representing correlations between SSR1 expression and immune inhibitor genes. (D) Heatmap showing correlations of SSR1 with immune stimulator genes. The color gradient in (C and D) reflects the strength and direction of correlations, with red indicating positive correlations and blue indicating negative correlations. $P < 0.05$.

expression might enhance resistance to these drugs (**Figure 7B**). **Figure 7C** presents results from STRING, predicting interactions between SSR1 and proteins encoded by other genes. SSR1 was found to strongly associated with SSR2, SSR3, SSR4, RPN1, and SEC61A1 (**Figure 7C**). These associations were further validated in **Figure 7D**, where the correlation of SSR1 expression with these genes was examined using the GEPIA2 database. High positive correlations were observed between SSR1 and SSR2 (R = 0.84), SSR3 (R = 0.91), RPN1 (R = 0.92), and a moderately positive correlation with SSR4 (R = 0.13) and SEC61A1 (R = 0.77), indicating a coordinated expression pattern between SSR1 and these genes in LIHC (**Figure 7D**).

Correlations of SSR1 with immune and molecular subtypes of LIHC

Correlations of SSR1 with immune and molecular subtypes as well as with immune-related genes were explored using TISIDB database. The analysis revealed that SSR1 expression varies significantly across immune and molecular subtypes of LIHC. In **Figure 8A**, SSR1 expression differs significantly among immune subtypes (C1 to C6), suggesting that SSR1 may play distinct roles within each immune context. Similarly, in **Figure 8B**, SSR1 expression significantly varies among molecular subtypes (iCluster 1 to 3), indicating that SSR1 expression is influenced by underlying molecular characteristics. Additionally, **Figure 8C**, **8D** highlights inter-

esting correlations between SSR1 and various immune inhibitor and stimulator genes, hinting at a potential involvement of SSR1 in immune suppression mechanisms.

Expression validation of SSR1 and its other associated genes on LIHC cell lines

The expression levels of SSR1 and its associated genes, predicted through the STRING database, were validated using RT-qPCR in two groups of cell lines: one group with seven LIHC cell lines and the other with three normal liver cell lines. Results showed that the expressions of SSR1 and its associated genes, including SSR2, SSR3, SSR4, RPN1, and SEC61A1 were significantly up-regulated in LIHC cell lines as compared to the normal controls (**Figure 9A**). Furthermore, ROC curves analysis was used to assess the diagnostic potential of these genes in distinguishing between LIHC and normal cells. Results showed that SSR1, SSR2, SSR4, RPN1, and SEC61A1 have AUC values of 1, indicating perfect sensitivity and specificity for distinguishing cancerous from normal cells (**Figure 9B**). In contrast, SSR3 has a lower AUC of 0.714, showing moderate diagnostic power compared to the other genes, which implies that it might not be as reliable a marker for this purpose (**Figure 9B**).

SSR1, SSR2, and SSR3 knockdown affects the proliferation and migration of LIHC cells

Finally, to examine the effect of SSR1, SSR2, and SSR3 on cell proliferation and migration, we transfected QGY-7703 and SMMC-7721 cell lines with siRNAs. **Figure 10A** confirmed a significant reduction in SSR1 expression in both QGY-7703 and SMMC-7721 cells at the mRNA level after transfection, while **Figure 10B**, **10C** and Supplementary Figure 1 showed reduce SSR1 protein levels via Western blot. Moreover, **Figure 10D** revealed a marked reduction in cell proliferation upon SSR1 knockdown in both cell lines. Similarly, **Figure 10E**, **10F** indicates a significant decrease in colony formation ability in the si-SSR1-transfected cells compared to controls. **Figure 10G**, **10H** presents wound-healing assay images and quantitative analysis, with panel H showing significantly enhanced wound closure in si-SSR1 cells as compared to controls, indicating increased migratory capability following SSR1 knockdown.

In **Figure 11**, SSR2 and SSR3 knockdowns in QGY-7703 cells show similar trends. **Figure 11A** confirmed effective SSR2 and SSR3 mRNA knockdown, and **Figure 11B**, **11C** and Supplementary Figure 1 showed corresponding protein level reductions. **Figure 11D** showed that both SSR2 and SSR3 knockdowns significantly inhibit cell proliferation. **Figure 11E**, **11F** displayed reduce colony formation in cells transfected with si-SSR2 and si-SSR3 compared to controls, highlighting the impact on cell growth potential. **Figure 11G**, **11H**, through the wound-healing assay, shows that knockdown of SSR2 and SSR3 reduced wound closure rates, indicating impaired cell migration.

Discussion

Liver hepatocellular carcinoma (LIHC), also known as hepatocellular carcinoma (HCC), is the most common form of liver cancer, accounting for over 90% of liver malignancies worldwide [28, 29]. It is a major global health concern, with an increasing incidence and mortality rate, particularly in regions with high prevalence of hepatitis B and C infections, chronic liver disease [30], and cirrhosis [6, 31]. According to recent epidemiological studies, LIHC ranks as the sixth most commonly diagnosed cancer and the third leading cause of cancer-related deaths globally [32, 33]. Despite advancements in diagnostic techniques and treatment modalities, the overall survival rate of LIHC patients remains low, primarily due to late-stage diagnosis and high recurrence rates after treatment [34, 35]. Therefore, identifying molecular markers that could aid in early diagnosis, predict prognosis, or provide therapeutic targets is essential to improving outcomes for LIHC patients [36, 37].

Signal sequence receptor 1 (SSR1), originally identified as part of the translocon complex involved in protein translocation across the endoplasmic reticulum, has recently gained attention for its potential role in cancer biology [38]. While SSR1 has been studied in various malignancies, its role in LIHC is less well characterized. Previous studies have linked SSR1 to cancer progression in other types of cancer, including colorectal cancer and breast cancer [39]. For instance, SSR1 has been shown to promote cancer cell proliferation and metastasis in breast cancer, while its overexpression has been correlated with poor prognosis in

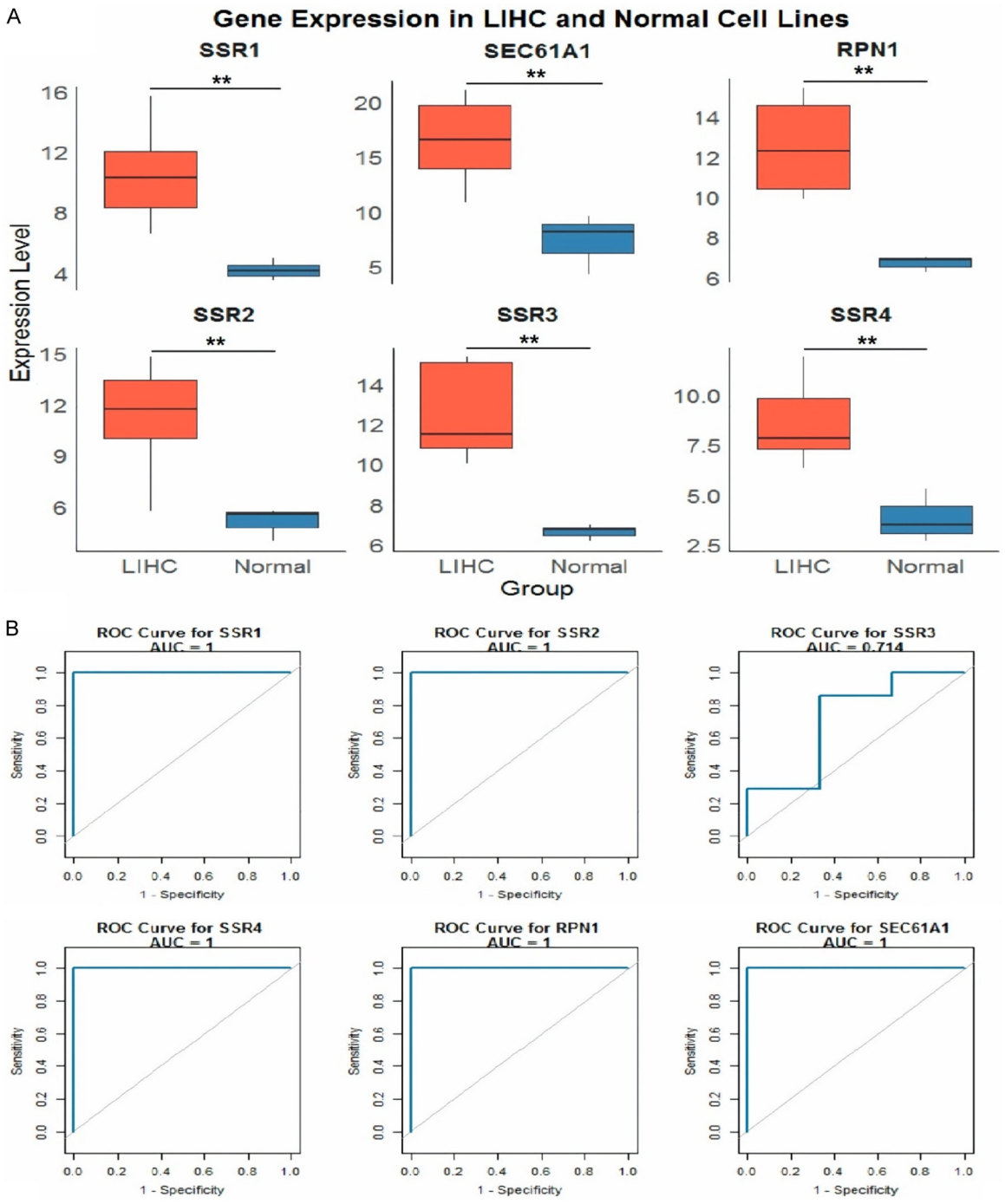

Figure 9. Gene expression analysis of signal sequence receptor subunit 1 (SSR1), SEC61 translocon subunit alpha 1 (SEC61A1), ribophorin 1 (RPN1), signal sequence receptor subunit 2 (SSR2), signal sequence receptor subunit 3 (SSR3), and signal sequence receptor subunit 4 (SSR4) in liver hepatocellular carcinoma (LIHC) and normal cell lines, and receiver operating characteristic (ROC) curve assessment. A. Gene expression levels of SSR1, SEC61A1, RPN1, SSR2, SSR3, and SSR4 were measured in LIHC and normal cell lines using real-time quantitative PCR (RT-qPCR). B. Receiver operating characteristic (ROC) curves were constructed to assess the diagnostic performance, measured by the area under the curve (AUC), of the SSR1, SSR2, SSR3, SSR4, RPN1, and SEC61A1 genes for distinguishing between LIHC and normal samples. **P < 0.01.

colorectal cancer [40, 41]. However, the functional role of SSR1 in LIHC has not been thoroughly investigated, and this study aims to bridge this gap.

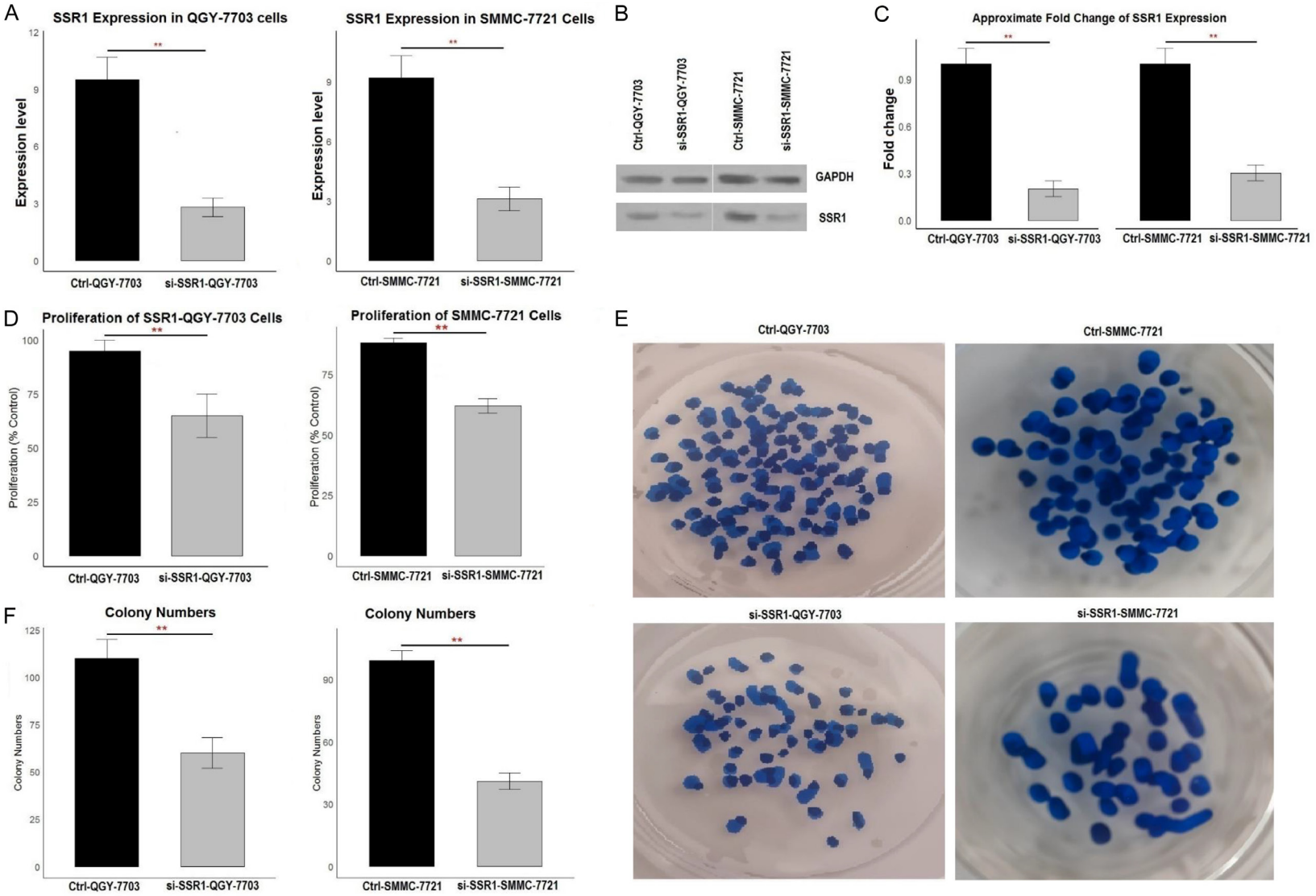
A
SSR1 Expression in QGY-7703 cells
Expression level
Ctrl-QGY-7703
si-SSR1-QGY-7703
SSR1 Expression in SMMC-7721 Cells
Ctrl-SMMC-7721
si-SSR1-SMMC-7721
B
Ctrl-QGY-7703
si-SSR1-QGY-7703
Ctrl-SMMC-7721
si-SSR1-SMMC-7721
GAPDH
SSR1
C
Approximate Fold Change of SSR1 Expression
Fold change
D
Proliferation of SSR1-QGY-7703 Cells
Proliferation (% Control)
Proliferation of SMMC-7721 Cells
E
Ctrl-QGY-7703
Ctrl-SMMC-7721
si-SSR1-QGY-7703
si-SSR1-SMMC-7721
F
Colony Numbers

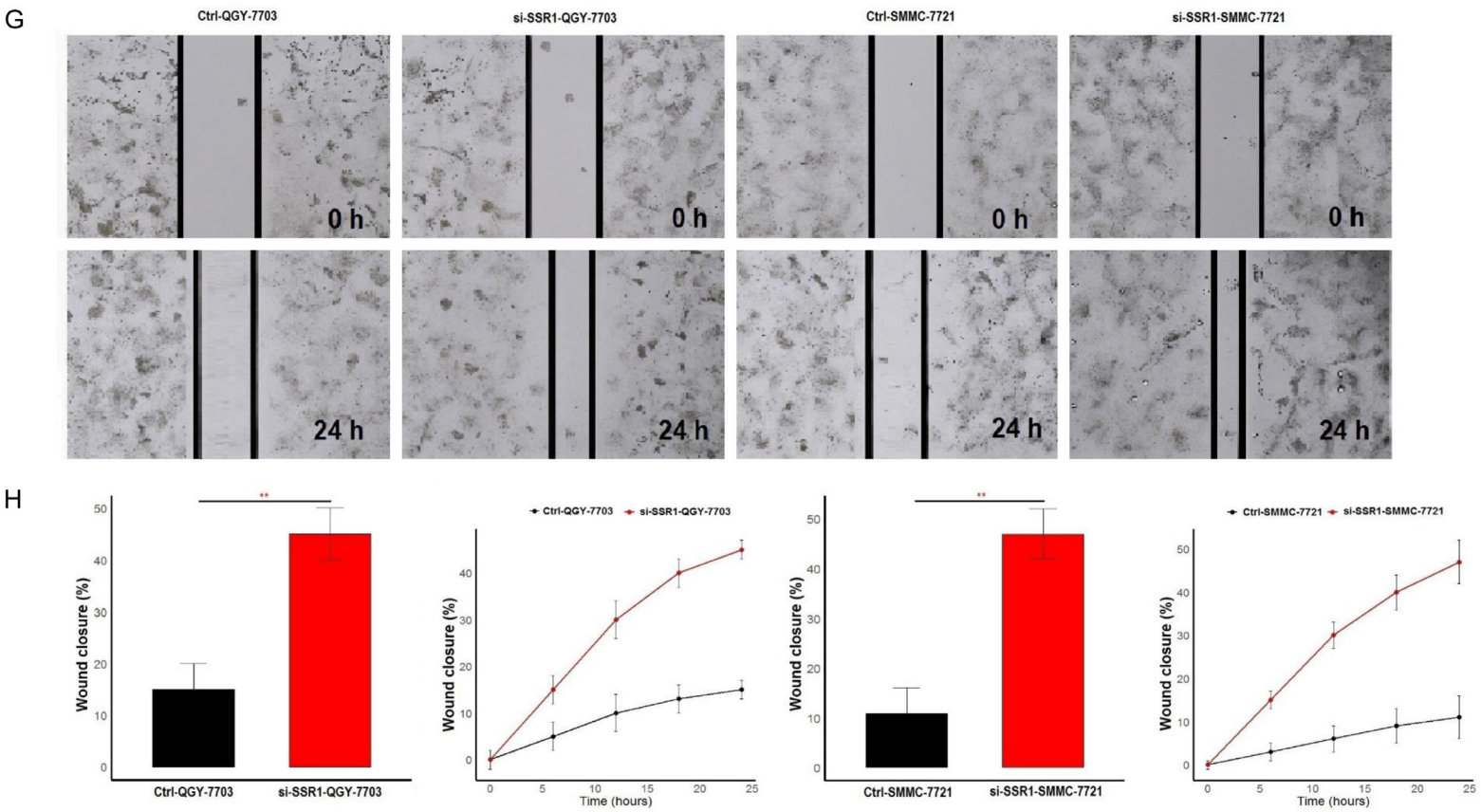

Figure 10. Effects of signal sequence receptor subunit 1 (SSR1) knockdown on the expression, proliferation, colony formation, and wound healing of QGY-7703 and SSMC-7721 cells. A. Real-time quantitative PCR (RT-qPCR)-based SSR1 expression was significantly reduced in QGY-7703 and SSMC-7721 cells transfected with SSR1 siRNA (si-SSR1-QGY-7703 and si-SSR1-SSMC-7721) compared to control cells (Ctrl-SSR1-QGY-7703 and Ctrl-SSMC-7721). B. Western blot expression analysis of SSR1 protein across si-SSR1-QGY-7703 and si-SSR1-SSMC-7721 cells and control cells. C. Down-regulation of SSR1 protein was observed in si-SSR1-QGY-7703 and si-SSR1-SSMC-7721 cells as compared to control cells. D. Cell proliferation was significantly decreased in the si-SSR1-QGY-7703 and si-SSR1-SSMC-7721 cells compared to the control cells. E. Colony formation assay showing a significant reduction in the number of colonies formed by si-SSR1-QGY-7703 and si-SSR1-SSMC-7721 cells compared to control cells. F. Representative images from the colony formation assay for si-SSR1-QGY-7703 and si-SSR1-SSMC-7721 and control cells. G. Wound healing assay showing the migration ability of si-SSR1-QGY-7703 and si-SSR1-SSMC-7721 cells and control cells at 0 and 24 hours. H. Bar and time-lapse graphs showed the quantification of the wound closure percentage, demonstrating that si-SSR1-QGY-7703 and si-SSR1-SSMC-7721 cells had a significantly increased wound closure rate compared to control cells. **P < 0.01.

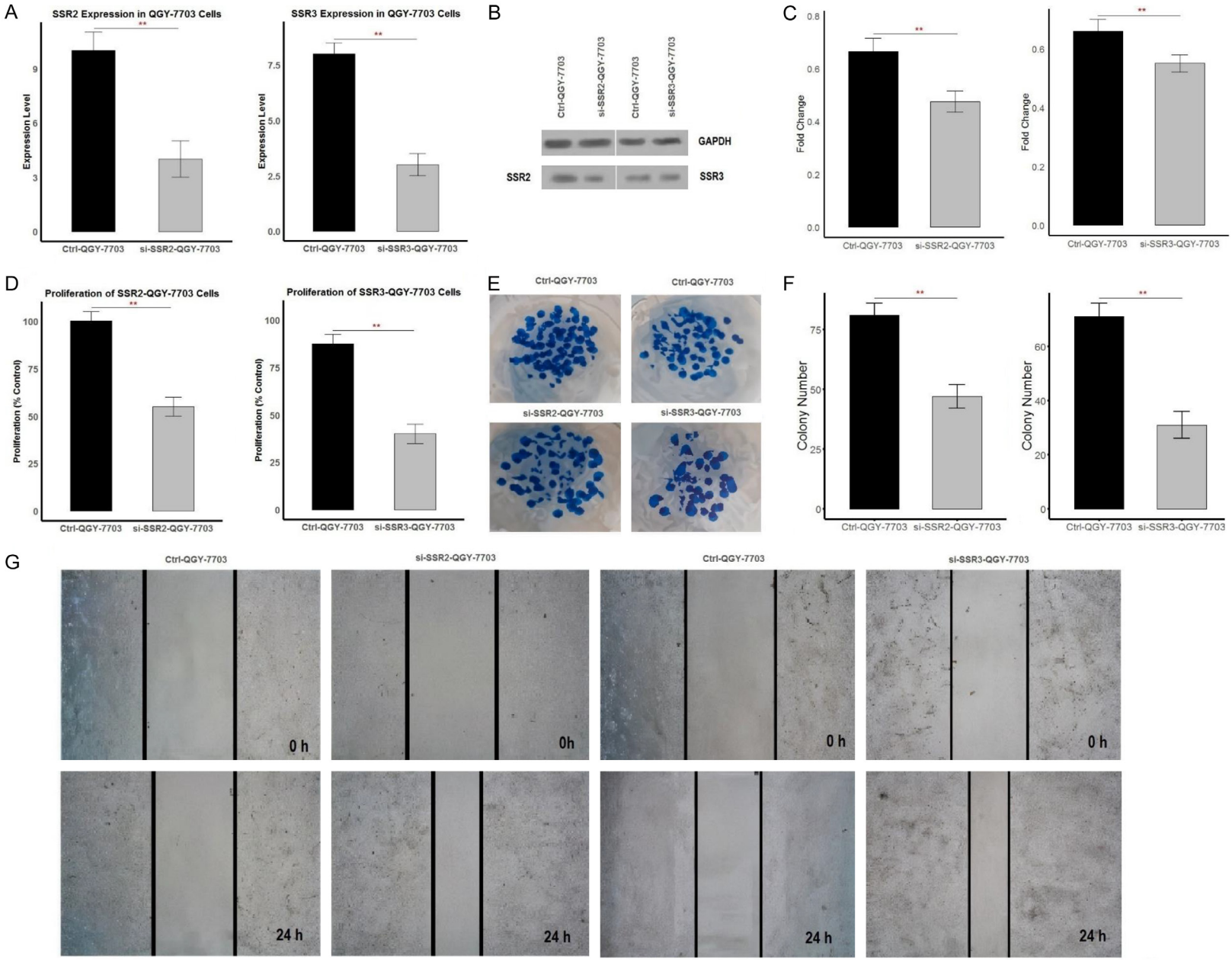
A
SSR2 Expression in QGY-7703 Cells
Expression Level
Ctrl-QGY-7703
si-SSR2-QGY-7703
SSR3 Expression in QGY-7703 Cells
Expression Level
Ctrl-QGY-7703
si-SSR3-QGY-7703
B
Ctrl-QGY-7703
si-SSR2-QGY-7703
Ctrl-QGY-7703
si-SSR3-QGY-7703
GAPDH
SSR2
SSR3
C
Fold Change
Ctrl-QGY-7703
si-SSR2-QGY-7703
Fold Change
Ctrl-QGY-7703
si-SSR3-QGY-7703
D
Proliferation of SSR2-QGY-7703 Cells
Proliferation (% Control)
Ctrl-QGY-7703
si-SSR2-QGY-7703
Proliferation of SSR3-QGY-7703 Cells
Proliferation (% Control)
Ctrl-QGY-7703
si-SSR3-QGY-7703
E
Ctrl-QGY-7703
Ctrl-QGY-7703
si-SSR2-QGY-7703
si-SSR3-QGY-7703
F
Colony Number
Ctrl-QGY-7703
si-SSR2-QGY-7703
Colony Number
Ctrl-QGY-7703
si-SSR3-QGY-7703
G
Ctrl-QGY-7703
si-SSR2-QGY-7703
Ctrl-QGY-7703
si-SSR3-QGY-7703
0 h
0h
0 h
0 h
24 h
24 h
24 h
24 h

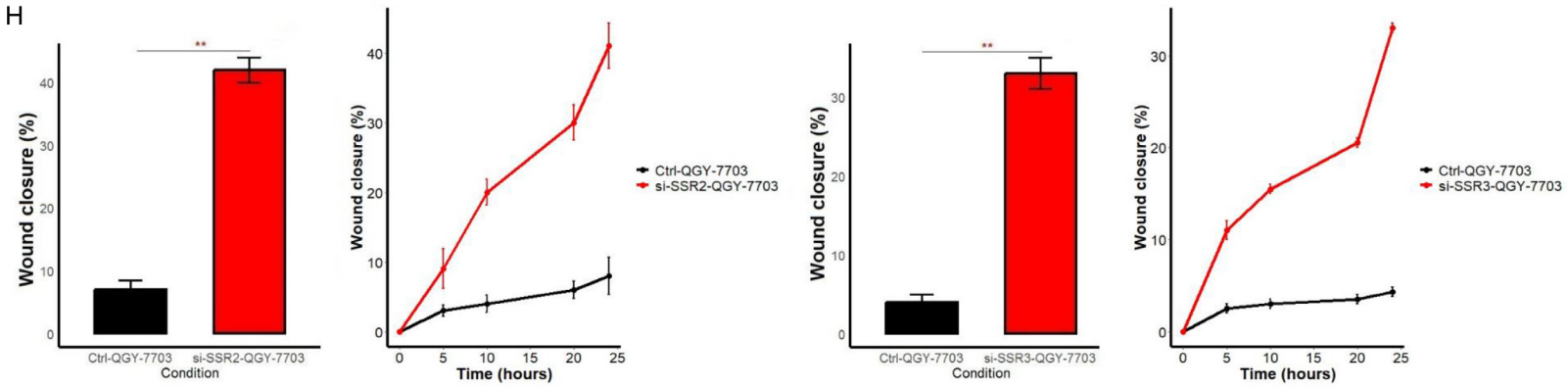

Figure 11. Effects of signal sequence receptor subunit 2 and 3 (SSR2 and SSR3) knockdown on the expression, proliferation, colony formation, and wound healing of QGY-7703 cells. A. SSR2 and SSR3 expression was significantly reduced in QGY-7703 cells transfected with SSR2 and SSR3 siRNAs (si-SSR2-QGY-7703 and si-SSR3-QGY-7703) compared to control cells (Ctrl-SSR2-QGY-7703 and Ctrl-SSR3-QGY-7703). B. Western blot expression analysis of SSR2 and SSR3 proteins across si-SSR2-QGY-7703 and si-SSR3-QGY-7703 cells and control cells. C. Down-regulation of SSR2 and SSR3 proteins was observed in si-SSR2-QGY-7703 and si-SSR3-QGY-7703 cells as compared to control cells. D. Cell proliferation was significantly decreased in the si-SSR2-QGY-7703 and si-SSR3-QGY-7703 groups compared to the control groups. E. Colony formation assay showing a significant reduction in the number of colonies formed by si-SSR2-QGY-7703 and si-SSR3-QGY-7703 cells compared to Ctrl-SSR2-QGY-7703 and Ctrl-SSR3-QGY-7703 cells. F. Representative images from the colony formation assay for Ctrl-SSR2-QGY-7703, si-SSR2-QGY-7703, Ctrl-SSR3-QGY-7703, and si-SSR3-QGY-7703 cells. G. Wound healing assay showing the migration ability of si-SSR2-QGY-7703 and si-SSR3-QGY-7703 cells and control cells at 0 and 24 hours. H. Bar and time-lapse graphs showed quantification of the wound closure percentage, demonstrating that si-SSR2-QGY-7703 and si-SSR3-QGY-7703 cells had a significantly increased wound closure rate compared to their respective control cells. **P < 0.01.

In this study, we performed a comprehensive analysis of SSR1 expression in LIHC, integrating transcriptomic and proteomic data from multiple sources. Our findings reveal a significant upregulation of SSR1 in LIHC tissues compared to normal liver tissues at both the mRNA and protein levels. These findings are consistent with reports in other cancer types, where SSR1 overexpression has been implicated in tumorigenesis [42]. Furthermore, promoter methylation analysis indicates that SSR1 is subject to promoter hypomethylation in LIHC, which likely contributes to its overexpression. This is in line with studies in colorectal cancer, where hypomethylation of SSR1 was also reported to drive its overexpression [43, 44]. Interestingly, our study highlights that SSR1 expression is not confined to LIHC alone but is upregulated in multiple other cancer types, as evidenced by the pan-cancer data. This raises the possibility that SSR1 may function as a pan-cancer marker, warranting further investigation in a broader range of cancers.

Mechanistically, SSR1 may contribute to LIHC progression by disrupting normal protein translocation processes at the ER, leading to ER stress and activation of the unfolded protein response (UPR) [45]. The ER plays a critical role in maintaining cellular homeostasis by ensuring proper folding and maturation of proteins [46]. Dysregulation of the ER's translocon complex, which includes SSR1, can result in an accumulation of misfolded proteins, triggering ER stress [47]. In response to this stress, cells activate the UPR, a survival mechanism that aims to restore ER homeostasis. However, chronic activation of the UPR has been linked to cancer progression, including tumor growth, survival, and metastasis [48]. In LIHC, SSR1 overexpression may lead to increased ER stress and chronic UPR activation, which can promote oncogenic signaling pathways [49]. The UPR can enhance cancer cell proliferation by activating pathways such as the PI3K/AKT and MAPK pathways, which are well-known to promote cell growth and survival [50]. Additionally, the UPR can inhibit apoptosis and increase autophagy, allowing cancer cells to survive under stressful conditions, such as nutrient deprivation or hypoxia, commonly found in the tumor microenvironment [51]. SSR1 may also influence LIHC progression through its interactions with the ER-associated degradation (ERAD) pathway [52]. The ERAD pathway is responsible for degrading misfolded proteins to maintain cellular homeostasis. Dysregulation of ERAD due to SSR1 overexpression can lead to the accumulation of oncogenic proteins or prevent the degradation of proteins that promote cancer progression [53]. This can result in sustained proliferative signaling and resistance to apoptosis, two hallmarks of cancer.

In addition to expression analysis, we examined the prognostic significance of SSR1 in LIHC. High SSR1 expression was associated with poor overall survival across different patient subgroups, including those with different tumor stages and histologic grades. These results align with previous studies in colorectal cancer, where high SSR1 expression was also linked to worse survival outcomes [54, 55].

Functional assays in this study demonstrated that SSR1, SSR2, and SSR3 knockdown significantly reduced the proliferation and colony-forming ability of LIHC cells, while enhancing cell migration, as observed in wound healing assays. This dual effect is intriguing and somewhat contrasts with previous findings in other cancers. For instance, in breast cancer, SSR1 and SSR2 knockdown has been reported to reduce both proliferation and migration, suggesting that the functional role of SSR1 may vary depending on the tumor context [41, 56]. In LIHC, it is possible that SSR1 primarily drives proliferation and survival, while its knockdown allows cells to adopt a more migratory phenotype, possibly as a compensatory mechanism. This observation is in line with studies showing that knocking down certain oncogenes can lead to increased cell migration due to cellular plasticity [41].

In terms of therapeutic implications, SSR1's overexpression and its role in promoting LIHC cell proliferation make it a promising candidate for targeted therapy. Our drug sensitivity analysis revealed potential interactions between SSR1 expression and sensitivity to certain tyrosine kinase inhibitors, such as Afatinib and Erlotinib, suggesting that SSR1 could be used as a biomarker to predict drug response. Moreover, the correlation between SSR1 expression and immune cell infiltration raises the possibility of targeting SSR1 in combination with immunotherapy, although further studies are needed to explore this avenue.

Conclusion

In conclusion, our study provides strong evidence that SSR1 is overexpressed in LIHC and plays a critical role in tumor progression. SSR1's potential as a diagnostic and prognostic marker, along with its role in cell proliferation and migration, emphasizes its importance in LIHC pathology. Future research should focus on elucidating the precise mechanisms by which SSR1 contributes to LIHC and other cancers, as well as exploring its potential as a therapeutic target.

Acknowledgements

This study was supported by 2023 Henan Provincial Key R&D and Promotion Special (Scientific and Technological Research) Project [grant numbers 232102310126] and The Henan Province Hospital of TCM Doctoral Research Fund [grant number 2021BSJJ04].

Disclosure of conflict of interest

None.

Address correspondence to: Chunzheng Ma, Henan Province Hospital of TCM, Zhengzhou 450002, Henan, China. E-mail: mczhnszyy666@126.com

References

[1] Li Q, Ding C, Cao M, Yang F, Yan X, He S, Cao M, Zhang S, Teng Y, Tan N, Wang J, Xia C and Chen W. Global epidemiology of liver cancer 2022: an emphasis on geographic disparities. Chin Med J (Engl) 2024; 137: 2334-2342.

[2] Guo P, Zeng M, Liu M, Zhang Y, Jia J, Zhang Z, Liang S, Zheng X and Feng W. Isolation of calenduloside E from achyranthes bidentata blume and its effects on LPS/D-GalN-induced acute liver injury in mice by regulating the AMPK-SIRT3 signaling pathway. Phytomedicine 2024; 125: 155353.

[3] Giraud J, Chalopin D, Blanc JF and Saleh M. Hepatocellular carcinoma immune landscape and the potential of immunotherapies. Front Immunol 2021; 12: 655697.

[4] Natu A, Singh A and Gupta S. Hepatocellular carcinoma: understanding molecular mechanisms for defining potential clinical modalities. World J Hepatol 2021; 13: 1568.

[5] Shabangu CS, Su WH, Li CY, Yu ML, Dai CY, Huang JF, Chuang WL and Wang SC. Systematic integration of molecular and clinical approaches in HCV-induced hepatocellular carcinoma. J Transl Med 2024; 22: 268.

[6] Han D, Ling B, Wu C and Jin H. The role of IQCB1 in liver cancer: a bioinformatics analysis. Transl Cancer Res 2024; 13: 5021-5036.

[7] Budhu A, Pehrsson EC, He A, Goyal L, Kelley RK, Dang H, Xie C, Monge C, Tandon M, Ma L, Revsine M, Kuhlman L, Zhang K, Baiev I, Lamm R, Patel K, Kleiner DE, Hewitt SM, Tran B, Shetty J, Wu X, Zhao Y, Shen TW, Choudhari S, Kriga Y, Ylaya K, Warner AC, Edmondson EF, Forgues M, Greten TF and Wang XW. Tumor biology and immune infiltration define primary liver cancer subsets linked to overall survival after immunotherapy. Cell Rep Med 2023; 4: 101052.

[8] Zampaglione L, Ferrari J, Vietti Violi N and Goossens N. The role of extrahepatic features on the development and management of hepatocellular carcinoma in steatotic liver disease. Discov Med 2024; 36: 1127-1138.

[9] Cai K, Fu W, Wang Z, Yang X, Liu H and Ji Z. Optimizing prognostic predictions in liver cancer with machine learning and survival analysis. Entropy (Basel) 2024; 26: 767.

[10] Yang H, Cheng J, Zhuang H, Xu H, Wang Y, Zhang T, Yang Y, Qian H, Lu Y, Han F, Cao L, Yang N, Liu R, Yang X, Zhang J, Wu J and Zhang N. Pharmacogenomic profiling of intra-tumor heterogeneity using a large organoid biobank of liver cancer. Cancer Cell 2024; 42: 535-551, e8.

[11] Zhang J, Zhang T, Guan G, Wen J, Chen CC, Liu J, Duan Y, Liu Y and Chen X. AUF1 promotes hepatocellular carcinoma progression and chemo-resistance by post-transcriptionally upregulating alpha-fetoprotein expression. Pathol Res Pract 2023; 245: 154441.

[12] Zaibaq F, Dowdy T and Larion M. Targeting the sphingolipid rheostat in gliomas. Int J Mol Sci 2022; 23: 9255.

[13] Qu J, Li M, Li D, Xin Y, Li J, Lei S, Wu W and Liu X. Stimulation of Sigma-1 receptor protects against cardiac fibrosis by alleviating IRE1 pathway and autophagy impairment. Oxid Med Cell Longev 2021; 2021: 8836818.

[14] Verhaegen M and Vermeire K. The endoplasmic reticulum (ER): a crucial cellular hub in flavivirus infection and potential target site for antiviral interventions. Npj Viruses 2024; 2: 24.

[15] Cao W, Li J, Hao Q, Vadgama JV and Wu Y. AMP-activated protein kinase: a potential therapeutic target for triple-negative breast cancer. Breast Cancer Res 2019; 21: 29.

[16] Irham LM, Wong HS, Chou WH, Adikusuma W, Mugiyanto E, Huang WC and Chang WC. Integration of genetic variants and gene network for drug repurposing in colorectal cancer. Pharmacol Res 2020; 161: 105203.

[17] Ichihara S, Toyooka S, Fujiwara Y, Hotta K, Shigematsu H, Tokumo M, Soh J, Asano H, Ichimu-

ra K, Aoe K, Aoe M, Kiura K, Shimizu K, Date H and Shimizu N. The impact of epidermal growth factor receptor gene status on gefitinib-treated Japanese patients with non-small-cell lung cancer. Int J Cancer 2007; 120: 1239-1247.

[18] Chandrashekar DS, Bashel B, Balasubramanya SAH, Creighton CJ, Ponce-Rodriguez I, Chakravarthi BVSK and Varambally S. UALCAN: a portal for facilitating tumor subgroup gene expression and survival analyses. Neoplasia 2017; 19: 649-658.

[19] Rhodes DR, Kalyana-Sundaram S, Mahavisno V, Varambally R, Yu J, Briggs BB, Barrette TR, Anstet MJ, Kincead-Beal C, Kulkarni P, Varambally S, Ghosh D and Chinnaiyan AM. Oncomine 3.0: genes, pathways, and networks in a collection of 18,000 cancer gene expression profiles. Neoplasia 2007; 9: 166-180.

[20] Li T, Fu J, Zeng Z, Cohen D, Li J, Chen Q, Li B and Liu XS. TIMER2.0 for analysis of tumor-infiltrating immune cells. Nucleic Acids Res 2020; 48: W509-W514.

[21] Thul PJ and Lindskog C. The human protein atlas: a spatial map of the human proteome. Protein Sci 2018; 27: 233-244.

[22] Tang G, Cho M and Wang X. OncoDB: an interactive online database for analysis of gene expression and viral infection in cancer. Nucleic Acids Res 2022; 50: D1334-D1339.

[23] Park SJ, Yoon BH, Kim SK and Kim SY. GENT2: an updated gene expression database for normal and tumor tissues. BMC Med Genomics 2019; 12 Suppl 5: 101.

[24] Liu CJ, Hu FF, Xie GY, Miao YR, Li XW, Zeng Y and Guo AY. GSCA: an integrated platform for gene set cancer analysis at genomic, pharmacogenomic and immunogenomic levels. Brief Bioinform 2023; 24: bbac558.

[25] Szklarczyk D, Gable AL, Nastou KC, Lyon D, Kirsch R, Pyysalo S, Doncheva NT, Legeay M, Fang T, Bork P, Jensen LJ and von Mering C. The STRING database in 2021: customizable protein-protein networks, and functional characterization of user-uploaded gene/measurement sets. Nucleic Acids Res 2021; 49: D605-D612.

[26] Tang Z, Kang B, Li C, Chen T and Zhang Z. GEPIA2: an enhanced web server for large-scale expression profiling and interactive analysis. Nucleic Acids Res 2019; 47: W556-W560.

[27] Ru B, Wong CN, Tong Y, Zhong JY, Zhong SSW, Wu WC, Chu KC, Wong CY, Lau CY, Chen I, Chan NW and Zhang J. TISIDB: an integrated repository portal for tumor-immune system interactions. Bioinformatics 2019; 35: 4200-4202.

[28] Rukmangad A, Deshpande A, Jamthikar A, Gupta D, Bhurane A and Meshram NB. Classification of H&E stained liver histopathology images using ensemble learning techniques for detection of the level of malignancy of hepatocellular carcinoma HCC. In editors. Adv Artif Intell-Empowered Decis Support Syst Papers in Honour of Prof John Psarras Springer 2024. pp. 89-108.

[29] Huang L, Li Y, Tang R, Yang P, Zhuo Y, Jiang X, Che L, Lin Y, Xu S, Li J, Fang Z, Zhao X, Li H, Yang M, Feng B, Wu D and Hua L. Bile acids metabolism in the gut-liver axis mediates liver injury during lactation. Life Sci 2024; 338: 122380.

[30] Hu M, Yuan X, Liu Y, Tang S, Miao J, Zhou Q and Chen S. IL-1β-induced NF-κB activation down-regulates miR-506 expression to promotes osteosarcoma cell growth through JAG1. Biomed Pharmacother 2017; 95: 1147-1155.

[31] Sun T, Lv J, Zhao X, Li W, Zhang Z and Nie L. In vivo liver function reserve assessments in alcoholic liver disease by scalable photoacoustic imaging. Photoacoustics 2023; 34: 100569.

[32] Hou Y, Li J, Yu A, Deng K, Chen J, Wang Z, Huang L, Ma S and Dai X. FANCI is associated with poor prognosis and immune infiltration in liver hepatocellular carcinoma. Int J Med Sci 2023; 20: 918-932.

[33] Zeng Q, Jiang T and Wang J. Role of LMO7 in cancer (Review). Oncol Rep 2024; 52: 117.

[34] Nong J, Yang K, Li T, Lan C, Zhou X, Liu J, Xie H, Luo J, Liao X, Zhu G and Peng T. SART3, regulated by p53, is a biomarker for diagnosis, prognosis and immune infiltration in hepatocellular carcinoma. Aging (Albany NY) 2023; 15: 8408-8432.

[35] Wang X, Yu C, Sun Y, Liu Y, Tang S, Sun Y and Zhou Y. Three-dimensional morphology scoring of hepatocellular carcinoma stratifies prognosis and immune infiltration. Comput Biol Med 2024; 172: 108253.

[36] Zhang YW, Zheng XW, Liu YJ, Fang L, Pan ZF, Bao MH and Huang P. Effect of oridonin on cytochrome P450 expression and activities in HepaRG cell. Pharmacol 2018; 101: 246-254.

[37] Jiang C, Xie N, Sun T, Ma W, Zhang B and Li W. Xanthohumol inhibits TGF-β1-induced cardiac fibroblasts activation via mediating PTEN/Akt/mTOR signaling pathway. Drug Des Devel Ther 2020; 14: 5431-5439.

[38] Tirincsi A, O'Keefe S, Nguyen D, Sicking M, Dudek J, Förster F, Jung M, Hadzibeganovic D, Helms V, High S, Zimmermann R and Lang S. Proteomics identifies substrates and a novel component in hSnd2-dependent ER protein targeting. Cells 2022; 11: 2925.

[39] Marinović S, Vuković K, Škrtić A, Poljak M, Petek S, Petek L and Kapitanović S. Epidermal growth factor receptor intron 1 polymorphism and microsatellite instability in sporadic colorectal cancer. Oncol Lett 2021; 21: 131.

[40] Ashbury JE, Lévesque LE, Beck PA and Aronson KJ. Selective serotonin reuptake inhibitor (SSRI) antidepressants, prolactin and breast cancer. Front Oncol 2012; 2: 177.
[41] Gwynne WD, Shakeel MS, Girgis-Gabardo A and Hassell JA. The role of serotonin in breast cancer stem cells. Molecules 2021; 26: 3171.
[42] Li J, Zhao Z, Wang X, Ma Q, Ji H, Wang Y and Yu R. PBX2-mediated circTLK1 activates JAK/STAT signaling to promote gliomagenesis via miR-452-5p/SSR1 axis. Front Genet 2021; 12: 698831.
[43] Buisine MP, Wacrenier A, Mariette C, Leteurtre E, Escande F, Aissi S, Ketele A, Leclercq A, Porchet N and Lesuffleur T. Frequent mutations of the CA simple sequence repeat in intron 1 of EGFR in mismatch repair-deficient colorectal cancers. World J Gastroenterol 2008; 14: 1053-9.
[44] Battaglin F, Jayachandran P, Strelez C, Lenz A, Algaze S, Soni S, Lo JH, Yang Y, Millstein J, Zhang W, Roussos Torres ET, Shih JC, Mumenthaler SM, Neman J and Lenz HJ. Neurotransmitter signaling: a new frontier in colorectal cancer biology and treatment. Oncogene 2022; 41: 4769-4778.
[45] Cao SS. Endoplasmic reticulum stress and unfolded protein response in inflammatory bowel disease. Inflamm Bowel Dis 2015; 21: 636-645.
[46] Chen X, Shi C, He M, Xiong S and Xia X. Endoplasmic reticulum stress: molecular mechanism and therapeutic targets. Signal Transduct Target Ther 2023; 8: 352.
[47] Klyosova E, Azarova I, Buikin S and Polonikov A. Differentially expressed genes regulating glutathione metabolism, protein-folding, and unfolded protein response in pancreatic β-cells in type 2 diabetes mellitus. Int J Mol Sci 2023; 24: 12059.
[48] Walczak A, Gradzik K, Kabzinski J, Przybylowska-Sygut K and Majsterek I. The role of the ER-induced UPR pathway and the efficacy of its inhibitors and inducers in the inhibition of tumor progression. Oxid Med Cell Longev 2019; 2019: 5729710.
[49] Pavlović N and Heindryckx F. Exploring the role of endoplasmic reticulum stress in hepatocellular carcinoma through mining of the human protein atlas. Biology (Basel) 2021; 10: 640.
[50] Morgos DT, Stefani C, Miricescu D, Greabu M, Stanciu S, Nica S, Stanescu-Spinu II, Balan DG, Balcangiu-Stroescu AE, Coculescu EC, Georgescu DE and Nica RI. Targeting PI3K/AKT/mTOR and MAPK signaling pathways in gastric cancer. Int J Mol Sci 2024; 25: 1848.
[51] Bonsignore G, Martinotti S and Ranzato E. Endoplasmic reticulum stress and cancer: could unfolded protein response be a druggable target for cancer therapy? Int J Mol Sci 2023; 24: 1566.
[52] Dong M, Bridges JP, Apsley K, Xu Y and Weaver TE. ERdj4 and ERdj5 are required for endoplasmic reticulum-associated protein degradation of misfolded surfactant protein C. Mol Biol Cell 2008; 19: 2620-2630.
[53] Taguchi K, Kaneko M, Motoike S, Harada K, Hide I, Tanaka S and Sakai N. Role of the E3 ubiquitin ligase HRD1 in the regulation of serotonin transporter function. Biochem Biophys Res Commun 2021; 534: 583-589.
[54] Chen L, Lin Y, Liu G, Xu R, Hu Y, Xie J and Yu H. Clinical value for diagnosis and prognosis of signal sequence receptor 1 (SSR1) and its potential mechanism in hepatocellular carcinoma: a comprehensive study based on high-throughput data analysis. Int J Gen Med 2021; 14: 7435-7451.
[55] Nie Y, Li D, Peng Y, Wang S, Hu S, Liu M, Ding J and Zhou W. Metal organic framework coated MnO2 nanosheets delivering doxorubicin and self-activated DNAzyme for chemo-gene combinatorial treatment of cancer. Int J Pharm 2020; 585: 119513.
[56] Liao Z, Zhang H, Su C, Liu F, Liu Y, Song J, Zhu H, Fan Y, Zhang X, Dong W, Chen X, Liang H and Zhang B. Long noncoding RNA SNHG14 promotes hepatocellular carcinoma progression by regulating miR-876-5p/SSR2 axis. J Exp Clin Cancer Res 2021; 40: 36.

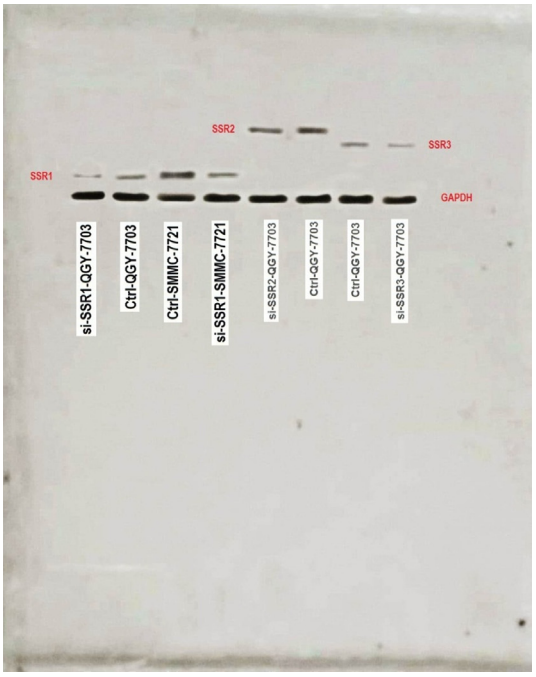

Supplementary Figure 1. Uncut western blot bands of SSR1, SSR2, and SSR3.